ORNL/TM-6956

GCFR Radial Blanket and Shield Experiment: Objectives, Preanalysis, and Specifications

D. T. Ingersoll
D. E. Bartine
F. J. Muckenthaler

OAK RIDGE NATIONAL LABORATORY
OPERATED BY UNION CARBIDE CORPORATION · FOR THE DEPARTMENT OF ENERGY

ORNL/TM-6956
Distribution Category UC-77

Contract W-7405-eng-26

Engineering Physics Division

GCFR RADIAL BLANKET AND SHIELD EXPERIMENT: OBJECTIVES, PREANALYSIS, AND SPECIFICATIONS

D. T. Ingersoll
D. E. Bartine
F. J. Muckenthaler

Date Published - September 1979

NOTICE. This document contains information of a preliminary nature. It is subject to revision or correction and therefore does not represent a final report.

OAK RIDGE NATIONAL LABORATORY
operated by
UNION CARBIDE CORPORATION
for the
DEPARTMENT OF ENERGY

TABLE OF CONTENTS

ABSTRACT

An integral experiment has been designed for the verification of radiation transport methods and nuclear data used for the design of the radial shield for the proposed 300 MW(e) gas-cooled fast breeder reactor (GCFR). The scope of the experiment was chosen to include a thorium oxide radial blanket mockup as well as several shield configurations in order to reduce the uncertainties in the calculated source terms for the radial shield, and to reduce the uncertainties in the calculated radiation damage to the prestressed concrete reactor vessel (PCRV). Additionally, the measurements are intended to bound the uncertainties in calculated gamma-ray heating rates within the blanket and shield. Although designed specifically for the GCFR, the experiment will provide generic data regarding deep penetration in ThO_2 and common shield materials, which should also benefit LMFBR designers.

Considerable preanalysis of the experiment was performed to solve design and fabrication problems. The analysis consisted of one-dimensional neutron and gamma-ray transport calculations in slab geometry representing the experimental configurations. Also, sensitivity calculations were performed for several of the detectors to be used in the experiments. Results showed that the detectors were highly sensitive to the nuclear cross sections of the materials which are of primary importance. Based on the intended objectives and the results of the preanalysis, a detailed measurement schedule was prepared which includes a description of configurations, detectors, and detector positions.

It was concluded that the final design and the measurement schedule is sufficient to meet the experiment objectives.

1.0. INTRODUCTION

The design of reactor shielding is a complex effort involving intimate relationships between radiation transport, thermomechanical forces, material properties, and economics. To aid the shield designer in achieving the optimum compromise of these considerations, several analytic tools have been developed such as discrete ordinates and Monte Carlo codes. For advanced reactors, where little operating experience is available, verification of these design methods and the design-based data is important. Integral experiments perform this function by (1) providing data against which the methods and data can be tested or (2) providing direct verification of the effectiveness of the final design.

An integral experiment has been designed for the verification of radiation transport methods and nuclear data used for the design of the radial shield for the proposed 300 MW(e) gas-cooled fast breeder reactor (GCFR).[1] The scope of the experiment was chosen to include a thorium oxide radial blanket mockup as well as several shield configurations. The blanket measurements are needed to reduce the large uncertainties which exist in the cross-section data required for calculating neutron transmission through a thorium blanket, hence reducing the uncertainties in the calculated source terms for the radial shield. Similarly, the shield measurements are needed to reduce the uncertainties in the calculated radiation damage to the prestressed concrete reactor vessel (PCRV). Additionally, the measurements are intended to bound the uncertainties in calculated gamma-ray heating rates within the blanket and shield. Although designed specifically for the GCFR, the experiment will provide generic data regarding deep penetration in ThO_2 and common shield materials, which should also benefit LMFBR designers.

With the relatively high cost of fabricating and performing large scale experiments, it was important that sufficient preanalysis be performed to produce a time- and cost-efficient experiment design and

BLANK PAGE

schedule. More importantly, some assurance had to be given that the results would satisfy the original intent of the experiment. For this integral test, it was desirable to design a one-dimensional mockup of the GCFR radial blanket and shield, and to provide sufficient flexibility for several alternate shield designs to be investigated. It was also necessary that the neutron source be representative of anticipated GCFR source spectra for both the blanket and the shield configurations. In addition, the materials, the dimensions, and the detectors and their locations had to be chosen so that the observed detector responses would be sufficiently sensitive to the quantities of interest in order to yield results which could be reliably extended to the GCFR design.

The experiment to be performed at the ORNL Tower Shielding Facility (TSF) will consist of measurements behind one-dimensional mockups of a GCFR-type radial blanket and radial shield. Both integral and spectral measurements will be made of the neutron and gamma-ray flux transmitted through successive materials and compared to corresponding calculations of the radiation transport. The need for such an experiment has been provided by the GCFR shield designer, General Atomic Company (GAC) in a document[2] which described desired results and the test requirements needed to achieve those results. In accordance with those requirements, a detailed description of the experiment design and specifications has been prepared and is presented in the following sections. The significant results from the preanalysis of the experiment will also be presented, followed by a statement of the Quality Assurance (QA) procedures to be used for the conduct and analysis of the experiment.

2.0. EXPERIMENT OBJECTIVES AND REQUIREMENTS

2.1 Conceptual Shielding Configuration I

Before defining the objectives and test requirements for the experiment, it is appropriate to first understand the reactor shield design from which the experiment was conceived. The reference downflow shield design is given in Fig. 2.1 and has been designated "Conceptual Shielding Configuration I" (CSC.I)[3]. Of primary interest for this experiment is the design of the radial shield at the core midplane level. Since the axial distribution of the neutron flux is a maximum at the midplane level, the composition and dimensions of the radial shield were determined largely from the shield's performance at the core midplane.

Table 2.1 lists the materials and dimensions of the reference radial shield design at the core midplane level. The design consists of two inner radial shield assemblies and a laminated outer shield assembly. Analysis by GAC showed that this combination of materials performed the best of all cases considered for meeting design criteria regarding nuclear heating rates, helium production, and total fluence exposures.

It is important to note tnat the final design for the GCFR demonstration plant does not exist, and hence the final radial shield design also does not exist. In particular, the recent decisions to require a lateral core restraint mechanism and to reverse the direction of helium flow may greatly alter the reference radial shield design. For example, the need to boronate the inner radial shield may be largely eliminated if the inner shield is cooled by inlet gas instead of outlet gas, as planned for the CSC.I design. This would result since the shield assemblies would be kept below the threshold temperature for thermal neutron-induced helium damage in the stainless steel. It is clear that considerable analyses of alternate shield designs will be required in the near future.

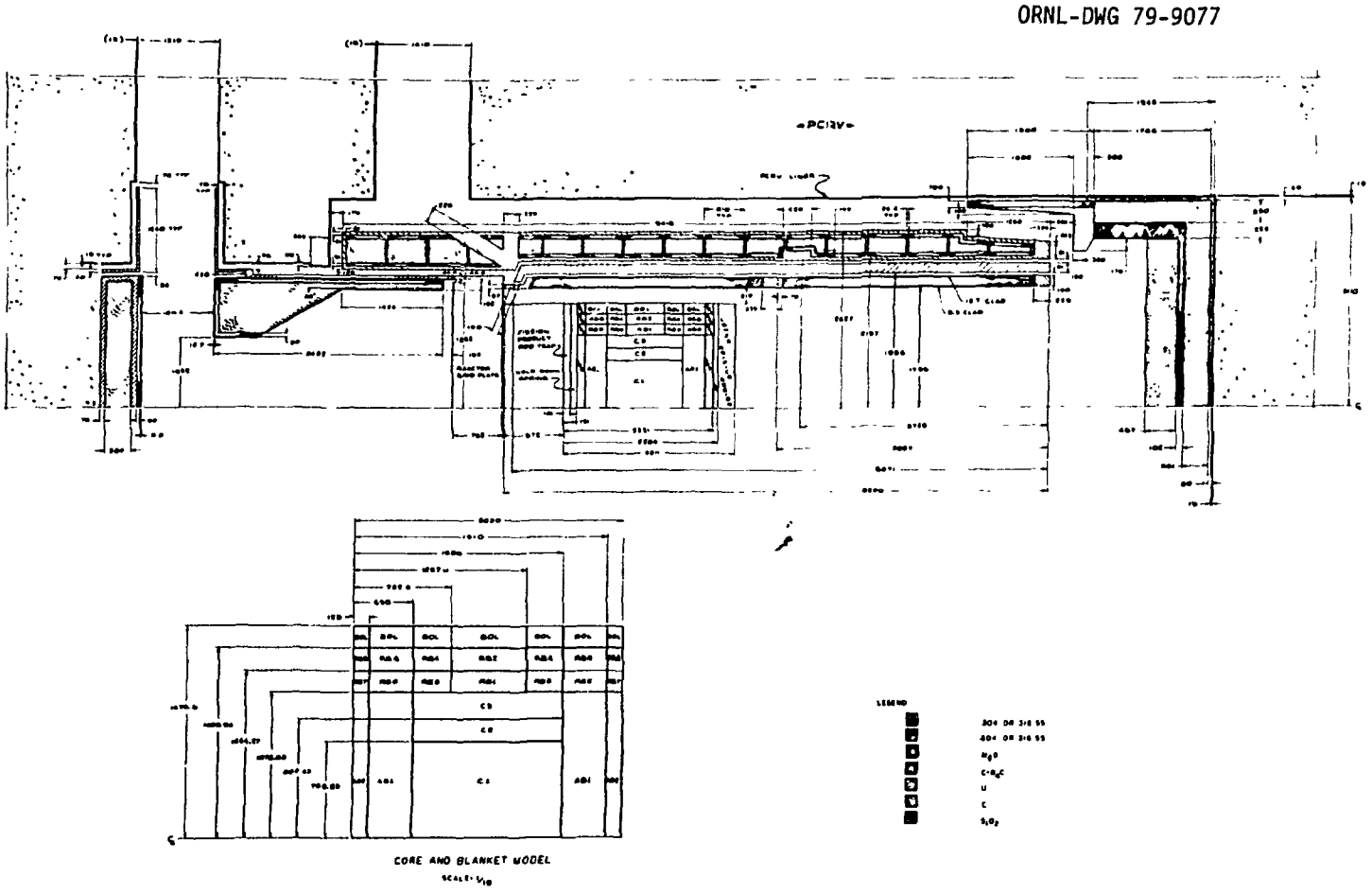

Fig. 2.1. Schematic of reference downflow GCFR shield design designated as "Conceptual Shielding Configuration I" (CSC.I) (Ref. 3). Also shown is the "Shielding Core Model A" (Ref. 4).

Table 2.1

Geometry and Materials for Conceptual Shielding Configuration I at the Core Midplane Level

Region and Material		Inner Radius (cm)	Outer Radius (cm)	Thickness (cm)
Core:	Enrichment Zone 1	0.0	77.9	77.9
	Enrichment Zone 2	77.9	96.9	19.0
	Enrichment Zone 3	96.9	115.6	18.7
Radial Blanket:	Row 1	115.6	134.1	18.5
	Row 2	134.1	152.6	18.5
	Row 3	152.6	171.0	18.4
Helium Gap		171.0	194.0	23.0
Inner Shield 1:	SS-316	194.0	195.0	1.0
	C + B_4C*	195.0	207.7	12.7
	SS-316	207.7	209.0	1.3
Helium Gap		209.0	214.1	5.1
Inner Shield 2:	SS-316	214.1	229.1	15.0
Helium Gap		229.1	234.2	5.1
Outer Shield:	SS-316	234.2	239.3	5.1
	C + B_4C*	239.3	244.4	5.1
	Graphite	244.4	267.0	22.6
	C + B_4C*	267.0	272.1	5.1
	SS-316	272.1	277.2	5.1
Helium Gap		277.2	312.9	35.7
PCRV Liner:	Fe	312.9	314.7	1.8
PCRV		314.7		

*25 weight-% boron mixture of graphite and B_4C at 1.6 g/ml bulk density.

The core and blanket model[4] used for the CSC.I design includes a UO_2 radial blanket; however, previous designs have used a ThO_2 blanket, and future designs may revert to ThO_2 blankets for political reasons. In either case, there are uncertainties in the UO_2 and ThO_2 cross section data, particularly regarding gamma-ray production and hence gamma-ray heating. Also, there are uncertainties in the Th data for deep neutron penetration. Indicative of the uncertainties in the Th data is the fact that the soon-to-be official ENDF/B-V evaluation for thorium contains a 15-30% lower capture cross section for neutron energies above 40 keV. This change will have significant impact on the calculation of the neutron and gamma-ray source from a GCFR Th blanket, and the calculation of the gamma-ray heating within the blanket.

2.2. Objectives and Requirements

Based on the design considerations described briefly in the previous section, ORNL and GAC cooperatively formulated the following specific objectives for the Radial Blanket and Shield Experiment:

1. To verify cross section data and transport methods used to calculate:
   a. the energy dependence of the neutron and gamma-ray flux through the radial blanket, radial shield, and PCRV
   b. the gamma-ray heating in the radial blanket and radial shield
   c. heterogeneous effects resulting from design complications in as-built shield designs.
2. To provide experimental comparisons of shield effectiveness for alternate shield designs.

In response to the objectives, GAC issued a report[2] presenting the test requirements for the experiment which were needed to insure that the objectives would be satisfied. The following list summarizes the requirements described in the GAC report.

1. The experimental configurations should contain blanket and shield assemblies which are representative of the current GCFR.
2. The assemblies should be modular to permit measurements on intermediate configurations, and to provide flexibility for constructing several alternate configurations.
3. The energy spectrum of the neutron source should be representative of a GCFR.
4. Measurements should include neutron and gamma-ray transmission measurements using spectral and integral detectors, and gamma-ray heating measurements using thermoluminescent detectors. High spatial resolution neutron detectors should be used for measurements of shield heterogeneities.
5. Sufficient preanalysis should be performed to insure the adequacy of the experiment design.
6. Sufficient postanalysis should be performed to provide: (a) several benchmark problems for the verification of new data and methods used for design analyses by ORNL and GAC, and (b) bias factors for radiation transmission and heating to be applied in actual design calculations.
7. Quality Assurance procedures should be consistent with 10 CFR 50, Appendix B, or ANSI N 45.2.

The purpose of the next two sections is to address the specific test requirements (excluding No. 6), and to show that within reasonable limits, all the requirements are satisfied by the final experiment design and measurement specifications.

3.0. PREANALYSTS

3.1. Calculation of GCFR Reference Shield Design

The preanalysis was initiated with a one-dimensional transport calculation of the CSC.I design (described in Sec. 2.1) from the core centerline to 30 cm into the PCRV at the level of the core midplane. The P_3S_8 cylindrical ANISN[5] calculation was run using the ORNL 51 neutron group and 25 gamma-ray group coupled cross section library which was prepared for GCFR shield analyses.[6] A distributed neutron source in the core and blanket regions was calculated using a 51-group neutron fission spectrum folded with the radial fission distribution resulting from a previous 2-D k-calculation (performed at GAC using the 2DB diffusion code). The neutron and gamma-ray flux spectra at several key locations in the design are given in Fig. 3.1 for neutrons, and in Fig. 3.2 for gamma rays. The spectra were used to guide the experiment design through the frequent comparison of the GCFR reference spectra with the spectra calculated for the TSF mockups.

3.2. Selection of a Spectrum Modifier

The neutron energy spectrum emerging from the TSF reactor[7] is not typical of a GCFR, so that a spectrum modifier (SM) is required to yield a source with the proper spectral characteristics. Several 1-D transport calculations were performed for various trial compositions of the SM, and the resulting SM neutron leakage was compared to the calculated neutron leakage from the CSC.I core. The selection of the best SM design was based on the visual comparison of spectra, and additional considerations of material obtainability, overall attenuation in the SM, and the relative importance of different energy ranges. The SM design, which was selected for use with the blanket mockups, was comprised of 10 cm carbon steel followed by 9 cm of aluminum and 2.5 cm of boral. Fig. 3.3 shows a comparison of the TSF leakage source, the modified spectrum, and the reference CSC.I core leakage.

BLANK PAGE

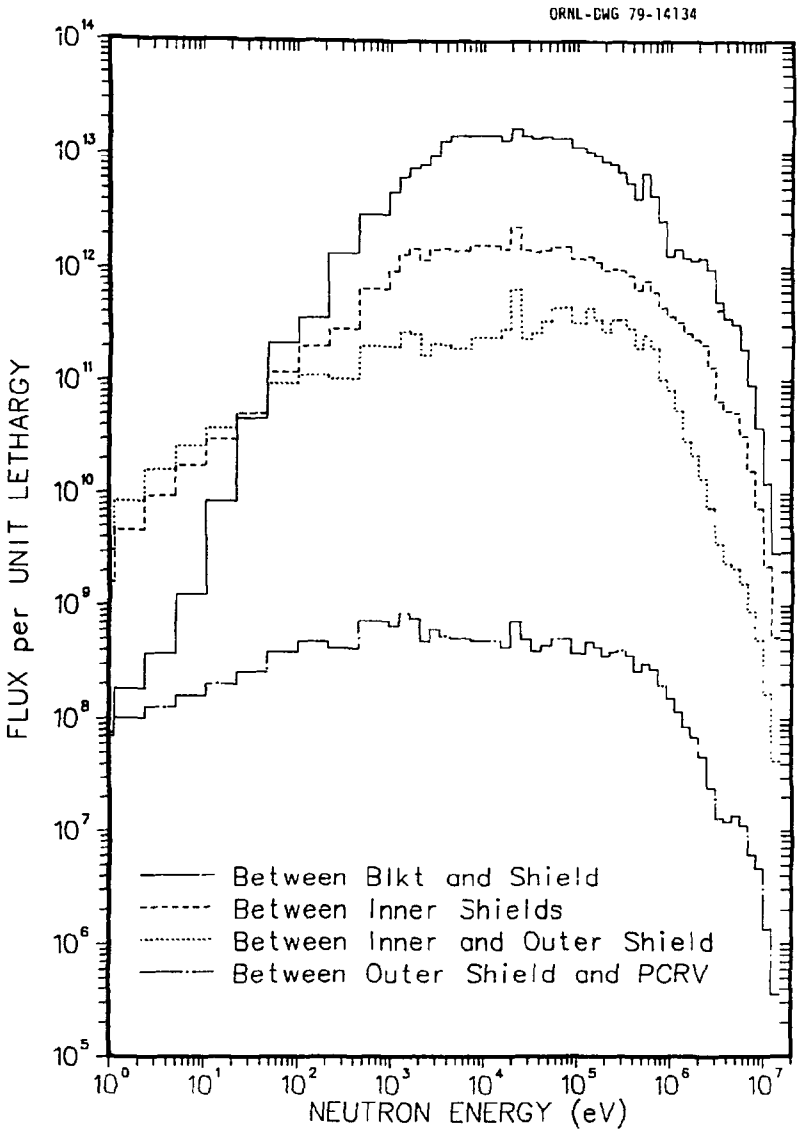

Fig. 3.1. Neutron energy spectra at selected locations in GCFR radial shield. Spectra calculated using 1-D CSC.I design model.

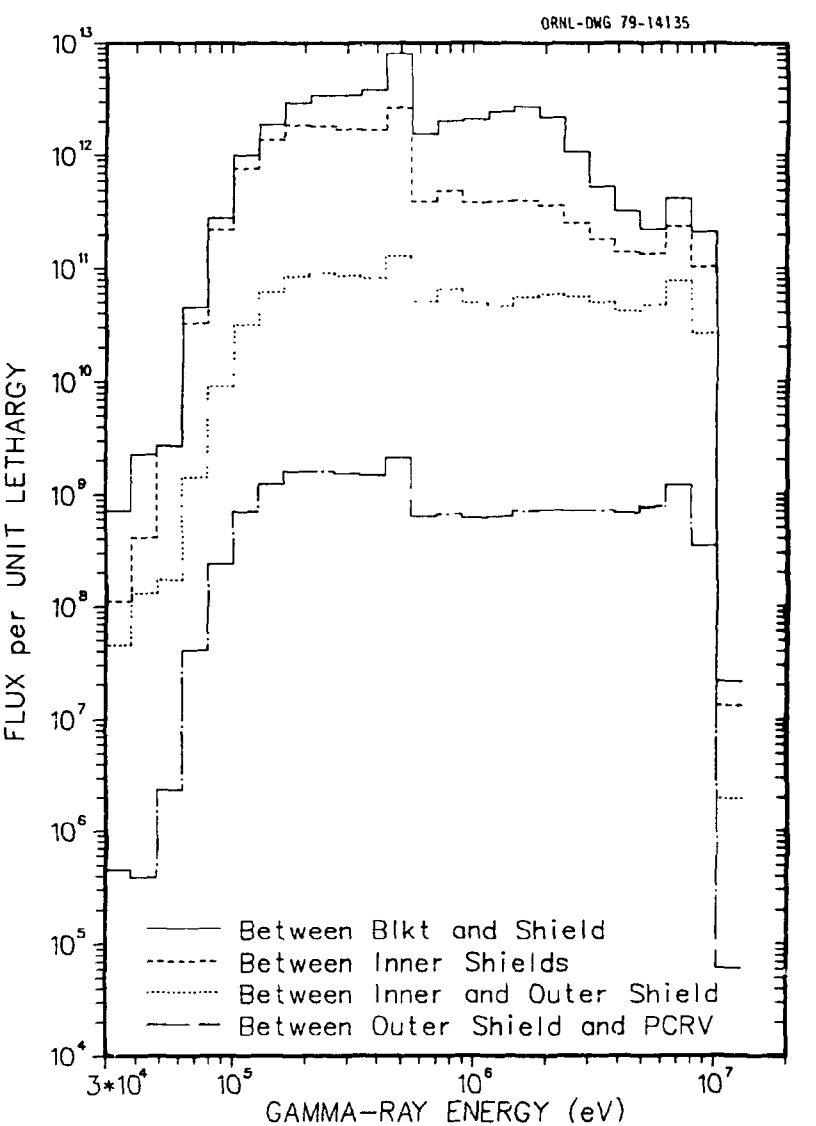

Fig. 3.2. Gamma-ray spectra at selected locations in GCFR radial shield. Spectra calculated using 1-D CSC.I design model.

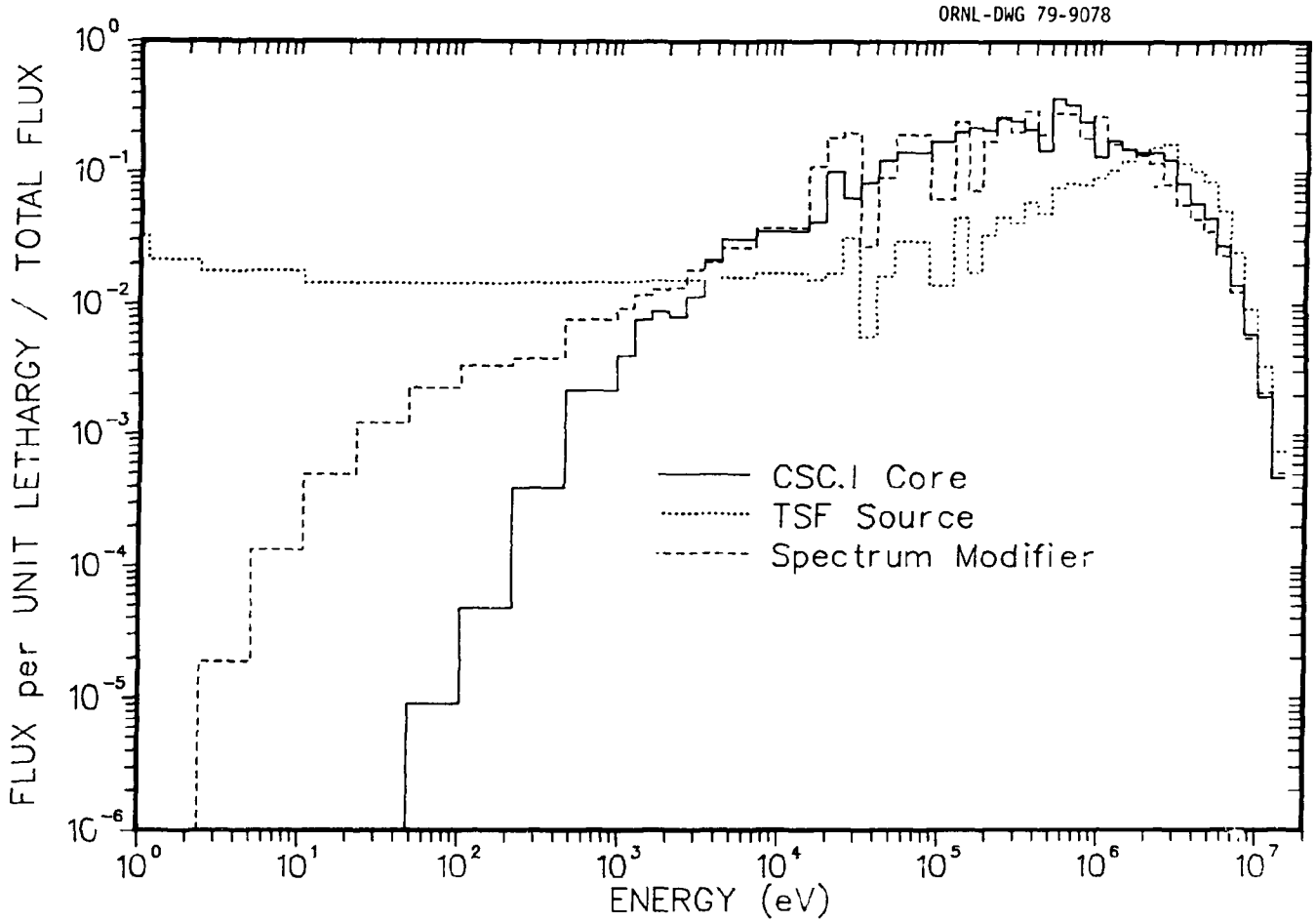

Fig. 3.3. Comparison of TSF reactor source, the spectrum emerging from the TSF spectrum modifier, and the neutron leakage from the GCFR reference core design.

ORNL-DWG 79-14136

ONE-DIMENSIONAL MODELS OF CONFIGURATIONS

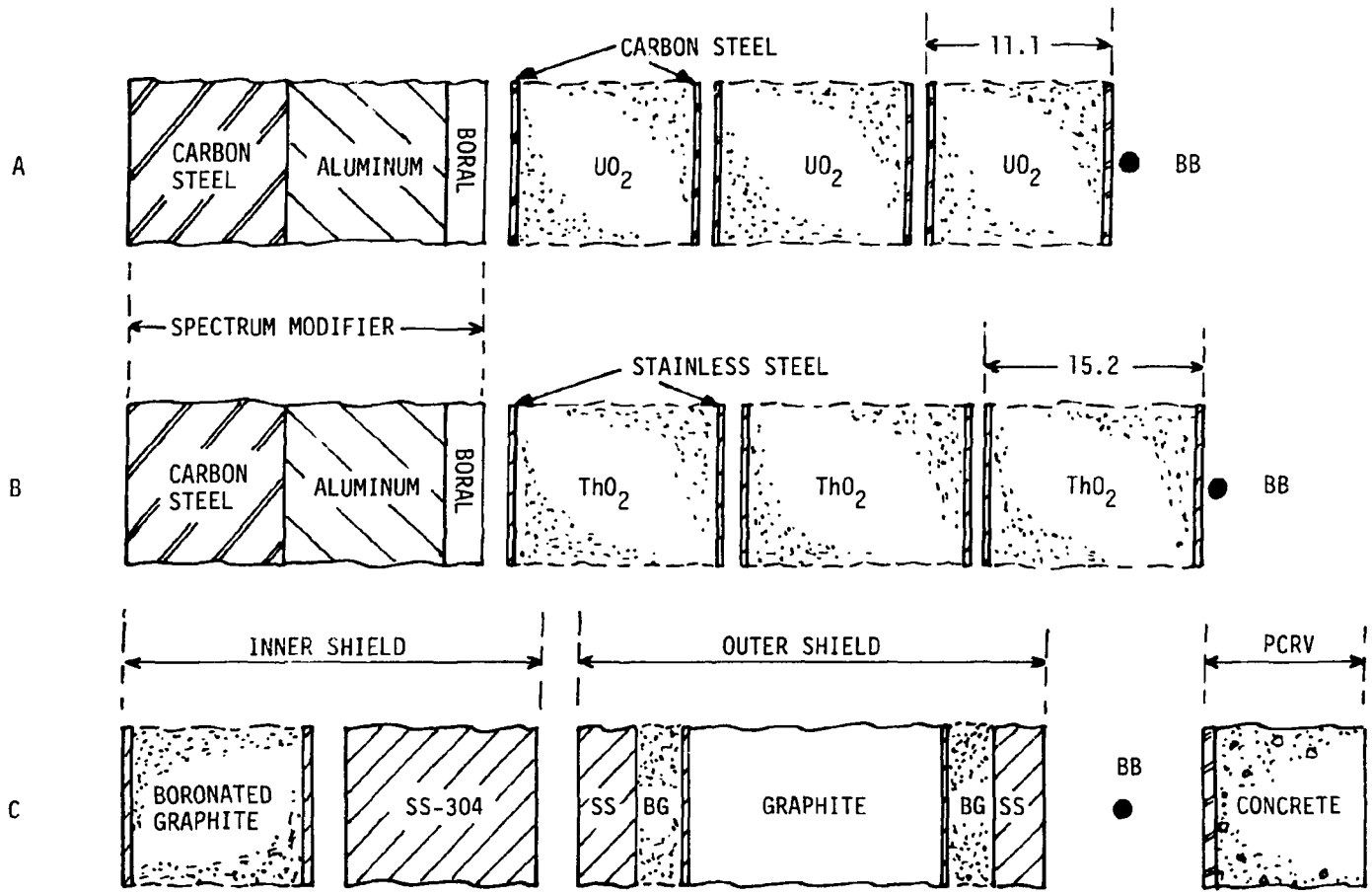

Fig. 3.4. One-dimensional models used for preanalysis. The slab calculations had a boundary source at the left boundary and a void on the right boundary.

3.3. Detector Sensitivities

An important aspect of the preanalysis phase of a data verification experiment is to assure that the detector measurements will be sufficiently sensitive to the data of interest so that reasonable and reliable conclusions can be made. The sensitivity analysis tools developed for shield design work equally well for experiment design and provide a maximum of information with a minimum of effort. The SWANLAKE sensitivity code[8], which uses forward and adjoint ANISN fluxes, was used numerous times in the preanalysis to determine detector sensitivities, sometimes resulting in design modifications.

The one-dimensional models used for the forward and adjoint calculations are shown in Fig. 3.4 which also shows the location of the calculated Bonner ball response. The TLDs are in-situ-type detectors and were located between the slab assemblies. In all three models, the boundary source was at the left boundary, and was the TSF neutron leakage source for the blanket mockups, and was the ThO_2 blanket leakage source (neutron and gamma ray) for the shield mockup. The nuclide densities for the materials used in the preanalysis calculations are given in Table 3.1.

3.3.1. TLD Response

The sensitivity of the thermoluminescent detector (TLD) used for gamma-ray heating measurements were calculated for both ThO_2 and UO_2 blanket mockups. The detector sensitivity to changes in nuclide densities were determined for the major nuclides in the blankets. Figure 3.5 shows the results for the case of a TLD located between the second and third ThO_2 blanket slabs. As shown in Fig. 3.5, the spectrum modifier used for the TLD 1-D calculations was somewhat different from the final SM design; however, the difference had only a slight effect on the sensitivity results.

Table 3.1

Nuclide Densities (atoms/barn-cm) of TSF Slabs Used in the Preanalysis Calculations for the GCFR Radial Blanket and Shield Experiment

	Boronated Graphite[a]	Graphite	Boral	Aluminum	SS-304	Carbon Steel	TSF Concrete	ThO_2[b]	UO_2
H							8.88-3		
Nat. B	2.23-2[c]		2.59-2						
C	6.02-2	8.83-2	6.45-3			9.82-4	7.97-3		
O							4.20-2	4.86-2	2.95-2
Na							2.73-5		5.19-3
Mg							1.44-3		
Al			3.65-2	6.05-2			4.14-4		7.05-3
Si							3.84-3		
S							1.02-4		
K							2.34-3		
Ca							1.00-2		
Cr					1.53-2				
Mn					1.76-3	1.55-3			
Fe			7.7-4	6.0-4	6.00-2	8.37-2	2.64-4		
Ni					7.80-3				
Th-232								2.43-2	
Nat. U									1.48-2

[a] For bulk density of 1.6 g/ml (95% of theoretical density).
[b] For bulk density of 10.0 g/ml; used in calculations at 7.0 g/ml.
[c] Read as "2.23×10^{-2}."

ORNL-DWG 79-14137

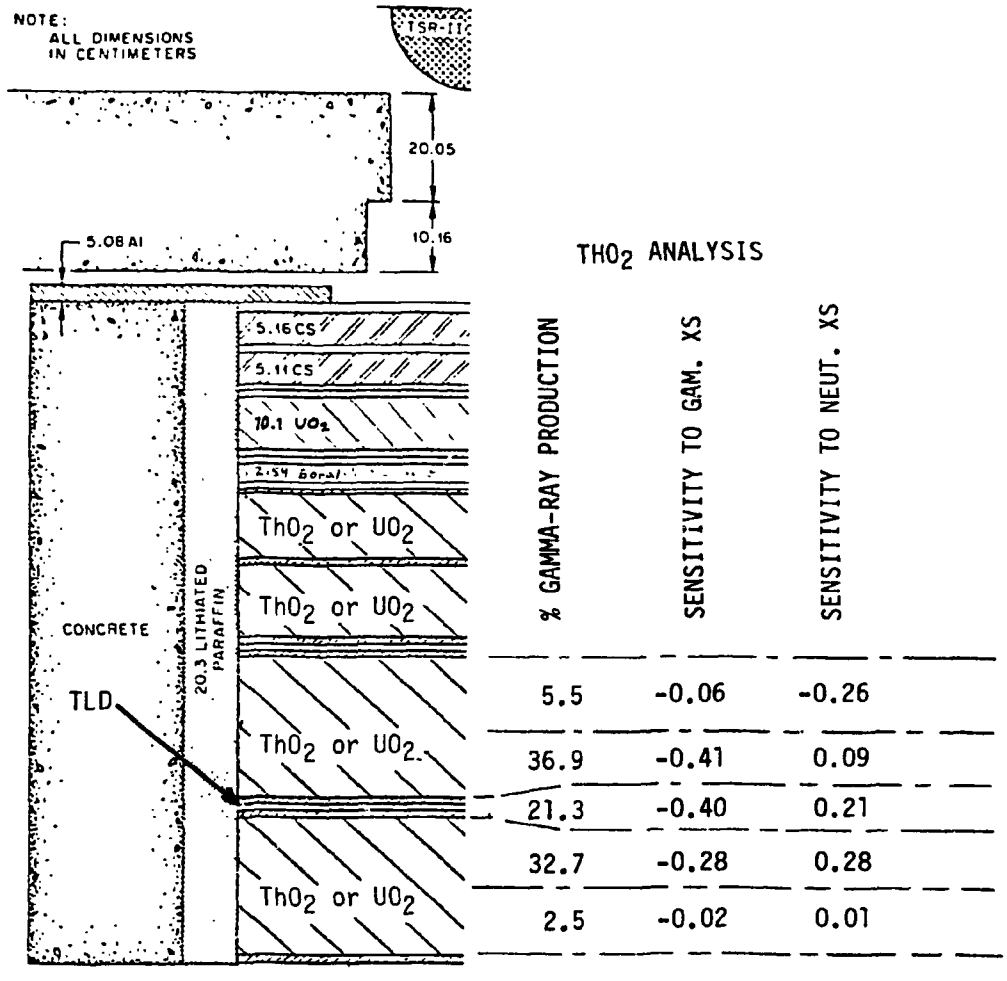

Fig. 3.5. Sensitivity of TLD to materials in ThO_2 blanket mockup.

ORNL-DWG 79-41438

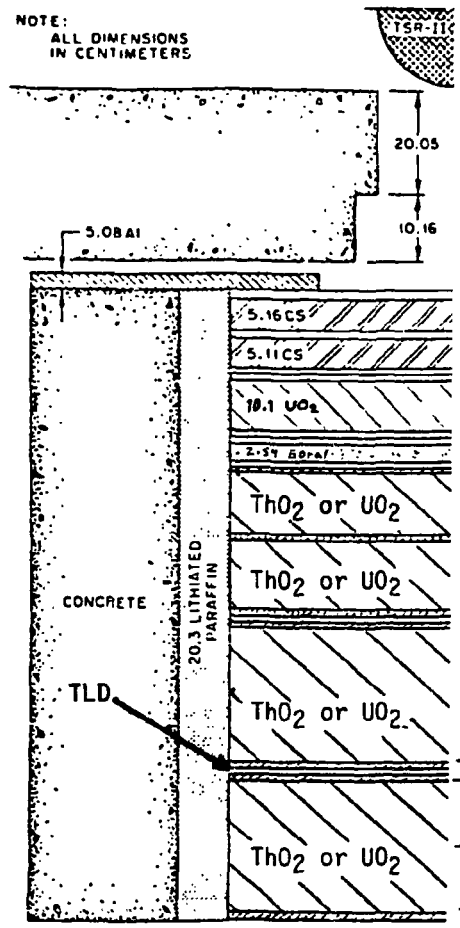

UO_2 ANALYSIS		
% GAMMA-RAY PRODUCTION	SENSITIVITY TO GAM. XS	SENSITIVITY TO NEUT. XS
3.5	-0.04	-0.24
31.2	-0.33	0.07
33.3	-0.41	0.33
29.6	-0.26	0.26
1.7	-0.0]	-0.02

Fig. 3.6. Sensitivity of TLD to materials in UO_2 blanket mockup.

The sensitivities given in Fig. 3.5 represent a percent change in the TLD response for a percent change in the density of the material in the indicated region. The results are given separately in terms of neutron and gamma-ray cross sections. The negative values indicate a dominance of the transport cross sections while the positive values reflect the importance of the neutron-induced gamma-ray production cross section. The sensitivities are not exceptionally large, but they seem adequate for reliable interpretation of the results.

An important result which is provided by the sensitivity code for the case of gamma-ray responses is the spatial distribution of neutron-produced gamma rays which contribute to the total detector response. Figure 3.5 shows that 21% of the TLD response resulted from gamma rays produced in the stainless steel immediately adjacent to the detector, while the remaining 79% resulted primarily from Th(n, γ) reactions inside the blanket slabs. Although this distribution appeared adequate for inferring the desired data regarding thorium gamma-ray production cross sections, the "background" due to the SS-304 gamma rays was further reduced by redesigning one of the three blanket slabs. Fabricating a full-width slab as two half-width slabs with a corresponding decrease in the SS-304 can thickness, allows less steel to border the TLD, hence reducing its contribution to the TLD response. It also allows neutron and gamma-ray transmission measurements to be made in finer blanket thickness increments.

Figure 3.6 gives the same results for a TLD in a UO_2 blanket mockup. The sensitivities are similar to the ThO_2 results, while the gamma-ray contributions show a greater importance for the steel. This result is likely due to a more realistic secondary gamma-ray multiplicity for uranium compared to the currently used thorium cross sections.

Table 3.2
Sensitivities of Bonner Ball Detectors
Located Behind ThO_2 Blanket Mockup

Region and Material		Sensitivity $[(\Delta R/R)/(\Delta\Sigma/\Sigma)]$ 3" BB	6" BB	10" BB
Blanket Row 1:	Th-232	-0.62	-0.64	-0.69
	O-16	-0.54	-0.61	-0.63
	SS-304	-0.14	-0.16	-0.18
Blanket Row 2:	Th-232	-0.74	-0.69	-0.71
	O-16	-0.42	-0.57	-0.62
	SS-304	-0.14	-0.16	-0.17
Blanket Row 3:	Th-232	-0.91	-0.79	-0.76
	O-16	-0.23	-0.45	-0.56
	SS-304	-0.19	-0.19	-0.19
Total:	Th-232	-2.28	-2.13	-2.16
	O-16	-1.19	-1.63	-1.81
	SS-304	-0.47	-0.51	-0.55

3.3.2. Bonner Ball Response

Bonner ball (BB) sensitivities were also calculated for the UO_2 and ThO_2 blanket mockups and the reference radial shield mockup. The sensitivities to the important nuclide densities were determined for the 3", 6", and 10" Bonner balls which represent epithermal, total, and fast neutron fluxes respectively. The detailed BB response functions are given in Sec. 4.2.

The calculated BB sensitivities are given in Tables 3.2 and 3.3 for the blanket configurations. In general, the sensitivities are quite large for the primary nuclides (thorium and uranium), and small for the less important materials. It is apparent, however, that the oxygen competes with the heavy metals in both the ThO_2 and UO_2 mockups, especially for the 10" BB. This implies that a careful consideration of both the heavy metals and the oxygen will be required for the final analysis of the experiment. Because the relative sensitivites to the heavy metals and the oxygen varies markedly between the 3" BB and the 10" BB, it should be possible to interpret final results in terms of deficiencies in either the heavy metal or the oxygen cross sections.

Table 3.4 gives the BB sensitivites for the radial shield mockup. As with the blanket mockups, the sensitivities are large which favors reliable interpretation of the experimental data. Also, the variation in relative sensitivity between the detectors should permit the identification of the materials which contribute to discrepancies between measurements and calculations, should any discrepancies be observed.

3.3.3. Gamma-Ray Flux at PCRV

Finally, sensitivities were calculated for a ficticious total gamma-ray detector located between the outer shield and PCRV mockups. The results are summarized in Table 3.5. The most significant conclusion from the calculation is the dominance of the steel in both the inner and

Table 3.3
Sensitivities of Bonner Ball Detectors
Located Behind UO_2 Blanket Mockup

Region and Material		Sensitivity $[(\Delta R/R)/(\Delta\Sigma/\Sigma)]$ 3" BB	5" BB	10" BB
Blanket Row 1:	Nat. U	-0.31	-0.33	-0.36
	Na	-0.05	-0.06	-0.06
	Al	-0.05	-0.06	-0.07
	O-16	-0.27	-0.32	-0.33
	C. Steel	-0.05	-0.06	-0.07
Blanket Row 2:	Nat. U	-0.39	-0.36	-0.37
	Na	-0.05	-0.06	-0.06
	Al	-0.03	-0.05	-0.06
	O-16	-0.21	-0.29	-0.32
	C. Steel	-0.05	-0.06	-0.07
Blanket Row 3:	Nat. U	-0.50	-0.42	-0.39
	Na	-0.04	-0.06	-0.06
	Al	-0.01	-0.04	-0.06
	O-16	-0.11	-0.24	-0.31
	C. Steel	-0.07	-0.07	-0.07
Total:	Nat. U	-1.20	-1.11	-1.12
	Na	-0.14	-0.18	-0.19
	Al	-0.09	-0.15	-0.19
	O-16	-0.59	-0.85	-0.95
	C. Steel	-0.17	-0.19	-0.21

Table 3.4
Sensitivities of Bonner Ball Detectors
Located Between Outer Shield and PCRV Mockups

Region and Material		Sensitivity $[(\Delta R/R)/(\Delta\Sigma/\Sigma)]$ 3" BB	6" BB	10" BB
Inner Shield 1:	SS-304	-0.31	-0.34	-0.37
	B	-0.31	-0.28	-0.26
	C	-0.73	-0.68	-0.65
Inner Shield 2:	SS-304	-1.86	-2.09	-2.30
Outer Shield:	SS-304	-1.16	-1.26	-1.36
	B	-0.76	-0.51	-0.39
	C (mix)	-0.56	-0.56	-0.55
	C (solid)	-2.78	-2.77	-2.67
PCRV Liner:	C. Steel	+0.07	+0.12	+0.10
PCRV:	TSF Conc.	+0.15	+0.08	+0.06
Total:	SS-304	-3.33	-3.69	-4.03
	B	-1.07	-0.79	-0.65
	C	-4.07	-4.01	-3.87
	C. Steel	+0.07	+0.12	+0.10
	TSF Conc.	+0.15	+0.08	+0.06

Table 3.5
Sensitivity $[(\Delta R/R)/(\Delta\Sigma/\Sigma)]$ of Total Gamma-Ray Flux
Between Outer Shield and PCRV Mockups

Region and Material		Secondary γ Contribution (%)	Sensitivity Σ (γ)	Sensitivity Σ (n)
Inner Shield 1:	SS-304	8.3	-0.18	-0.11
	B	0.1	-0.03	-0.28
	C	0.3	-0.11	-0.53
Inner Shield 2:	SS-304	22.3	-1.41	-0.98
Outer Shield:	SS-304	44.7	-2.14	-0.01
	B	13.5	-0.06	-0.30
	C (mix)	0.1	-0.17	-0.17
	C (solid)	1.3	-0.65	-0.45
PCRV Liner:	C. Steel	8.7	-0.05	+0.03
PCRV:	TSF Conc.	2.0	-0.01	+0.15
Total:	SS-304	75.3	-3.73	-1.10
	B	13.6	-0.09	-0.58
	C	1.7	-0.93	-1.15
	C. Steel	8.7	-0.05	+0.03
	TSF Conc.	2.0	-0.01	+0.15

outer shield slabs. It is interesting that almost 10% of the response is due to the Fe liner located "behind" the detector. Also, the secondary gamma-ray contributions sum to 100%, i.e., the total detector response, which means that source gamma-rays from the ThO_2 blanket source were effectively attenuated by the shield.

Actually, the contributions totaled nearly 102%, and summed to over 117% in an earlier attempt. The impossible value of 117% was improved to the more realistic 102% by grossly refining the mesh spacing near the detector. This was required in order to give a proper treatment of the source for the adjoint calculation which was the total gamma-ray flux. The largest contributor to the error was an overprediction of the importance of low energy gamma rays produced in boron in the boronated graphite region nearest the detector (see Fig. 3.4). It is expected that a further refinement of the mesh would bring the sum of all gamma-ray contributions to a value of 100%.

3.4. Contributon Analysis

While the sensitivity analysis provides a quantitative assessment of the importance of individual materials, it is sometimes useful to obtain a qualitative assessment of the importance of various components in an experimental configuration. Contributon theory[9] provides this information by allowing one to calculate at every spatial point in the configuration the flux of particles (called contributons) which contribute to an observed response, e.g., a detector count. For one-dimensional problems, one can determine the contributon flux for each energy group at every spatial location. The TOOTH code (1-D equivalent of the more popular FANG code[10]) was prepared for the purpose of calculating the space-energy contributon flux and plotting the flux as a projected 3-D surface. Since the TOOTH code requires only the forward and adjoint ANISN fluxes, which were already required for the sensitivity calculations, several TOOTH plots were generated for the radial blanket and shield configurations. A few sample cases are described below.

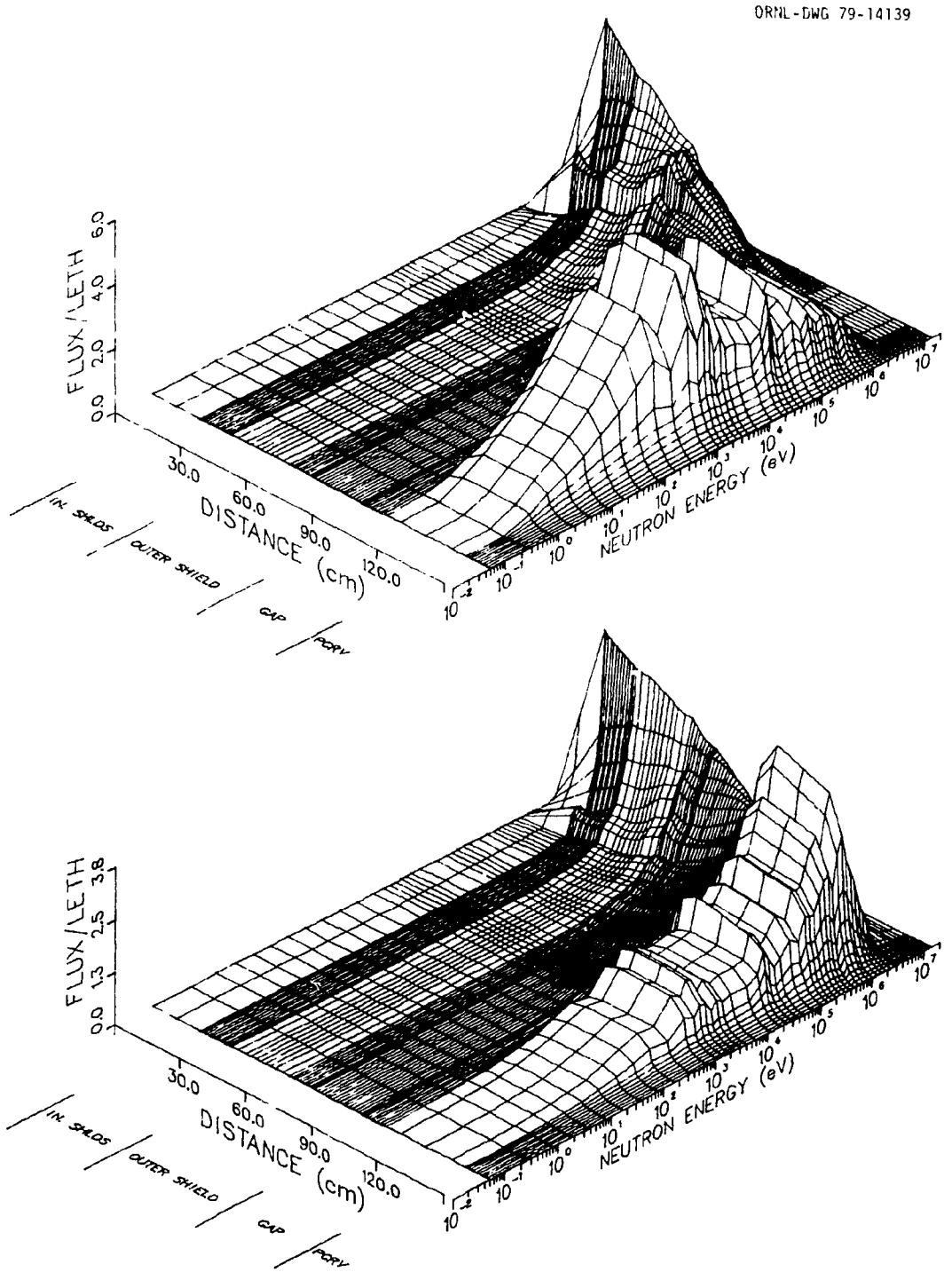

Fig. 3.7. Contributon flux ($\phi^*\phi$) for 3" Bonner ball (above) and 10" Bonner ball (below) located in gap between the outer shield and the PCRV.

Figure 3.7 compares the contributon surfaces for a 3" BB and a 10" BB located in the gap between the outer shield mockup and the simulated PCRV. The source for the forward calculation was the neutron leakage from the ThO_2 blanket configuration. An attempt was made in Fig. 3.7 to indicate the approximate location of the significant shield components. The two surfaces appear quite similar for the inner and outer shield regions, owing to the fact that only the high-energy source neutrons can survive the attenuation through the boronated shield sections. Near the detector position, however, the two surfaces differ which is a reflection of their particular energy response. The 3" BB emphasizes the lower energy neutrons which are generated in the final steel layer of the outer shield and also neutrons scattered back from the concrete. The 10" BB observes primarily the source neutrons slightly modified by the final layer of steel in the outer shield.

Neutron-only problems like the ones just described are relatively straightforward to interpret. Coupled neutron-gamma-ray problems provide a greater challenge, especially when considering the neutron contributon flux for a gamma-ray response. Such a case is shown in Fig. 3.8 which shows the neutron contributon flux in the shield mockup due to the ThO_2 blanket source. However, for this problem, the observed response is the total gamma-ray-flux detector located between the shield and the PCRV. Nearly all types of gamma-ray production processes appear to be represented in this example, from inelastic scattering to thermal neutron capture. The dominant peak in the distant corner of the figure is likely due to the large number of high-energy source neutrons contributing inelastic gamma-rays, while the local peaks throughout the shield are due to intermediate energy neutron capture in the stainless steel. At low neutron energies, both the outer shield graphite and the PCRV concrete contribute thermal capture gamma-rays.

Figure 3.9 shows the gamma-ray contributon flux for the same problem described above. The surface is less dramatic than the previous one, but is does show a few features of gamma-ray transport cross sections.

ORNL-DWG 79-14140

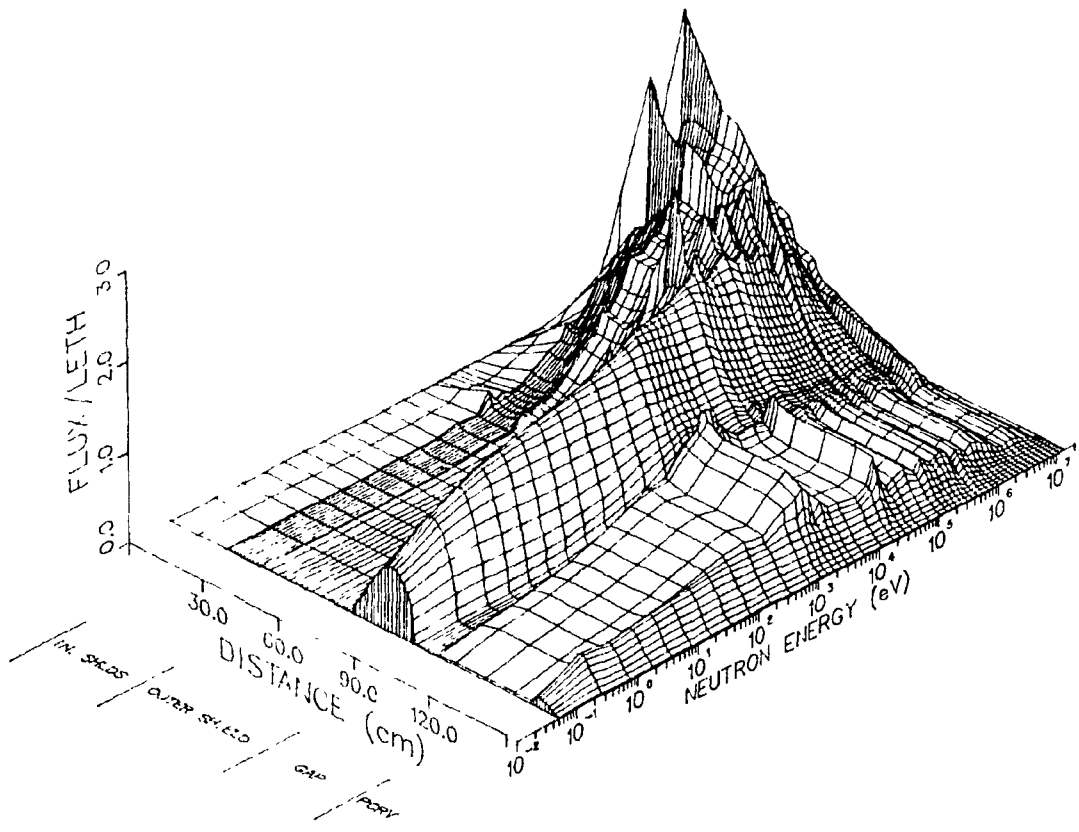

Fig. 3.8. Contributon flux for total gamma-ray flux detector located between outer shield and PCRV mockup. The surface represents neutron contributons and is dominated by gamma-ray production processes.

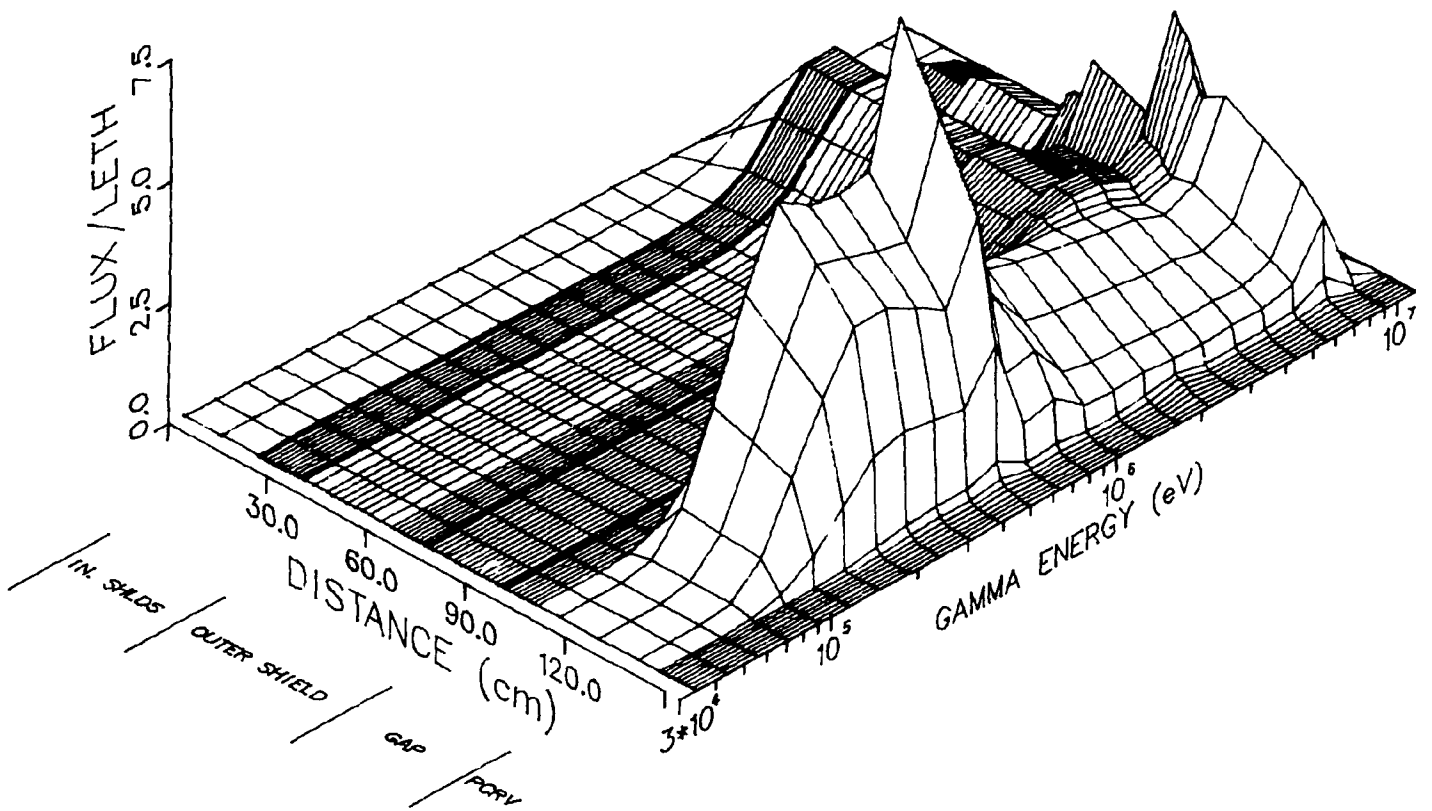

Fig. 3.9. Contributon flux for total gamma-ray flux detector located between outer shield and PCRV mockup. The surface represents gamma-ray contributons and is dominated by gamma-ray transport processes.

The characteristic minimum in the photon interaction cross section appears as the ridge through the shield near 3 MeV. Also the 7-8 MeV neutron-capture gamma ray from the steel, and the 0.511 MeV annihilation gamma ray appear in the surface.

Although the value of the contributon analysis may seem vague for the purpose of preanalysis, the method should help to identify the source of disagreement between calculations and measurements, should any disagreements be observed.

3.5. Special Problems Requiring Analysis

In every experiment, no matter how simply conceived or how carefully thought out, problems are encountered during the design, fabrication and performance stages. Most problems which arise require a rapid evaluation of alternatives to avoid costly delays. The same tools used in the routine preanalysis usually provide the means for a quick solution to the special problems. Three of the more significant problems encountered with the Radial Blanket and Shield Experiment are described below.

3.5.1. Lack of Clean UO_2

The original intent was to include in the blanket phase of the experiment a duplicate set of measurements on UO_2 blanket mockups and ThO_2 mockups. However, insufficient amounts of UO_2 were readily available, which left primarily three alternatives: (a) UO_3 available at Savannah River (SRP) could be fabricated into suitable slabs, (b) previously fabricated CRBR-type UO_2 slab available at the TSF could be used, or (c) the UO_2 blanket measurements could be discarded. Whereas the CRBR-type blankets contain some sodium and aluminum, the SRP UO_3 contains significant amounts of water and nitrates. Calculations were performed to evaluate the acceptability of either alternative, and it was concluded that neither the CRBR-type UO_2 or the SRP UO_3 material

was satisfactory for the "benchmark-type" comparison with ThO_2 that was intended. It was therefore decided to reduce the UO_2 measurements to only two configurations utilizing the CRBR-type assemblies.

Determining that a substitute material is adequate or inadequate usually involves subjective comparisons of the substitute with the intended material. Figure 3.10 compares the calculated neutron leakage from three different UO_2 blanket mockups. Included in Fig. 3.10 are the intended "clean" UO_2 case and the two alternatives: the SRP stock UO_3 and the CRBR-type assemblies. Except for a dip in the leakage spectrum corresponding to a sodium broad resonance, the CRBR-type assemblies compare favorably with the desired UO_2 case. However, the SRP UO_3 material yielded a considerable spectral shift. Also, an error was discovered in the SRP calculation: the UO_3 was mixed with 1 volume-% water instead of the actual 1 weight-% water, which would result in an even worse spectral shift. Furthermore, the theoretical density of UO_3 is much less than UO_2, which would have required that the blanket slabs be fabricated with a correspondingly greater thickness.

It was therefore decided that no UO_2 assemblies should be fabricated and that data from previous TSF experiments which used the CRBR-type UO_2 slabs would be used for the analysis. It was also decided to include a few key measurements in this experiment using the UO_2 slabs for an intercomparison with the previous experiments, and also for measurements through the shield mockup with a UO_2 blanket source.

3.5.2. Density of Boronated Graphite

Portions of the GCFR radial shield design utilize a boronated graphite mixture containing 25 weight percent (w/o) boron and having a bulk density of 1.6 g/cc. It was initially believed that a 25 w/o B mixture of graphite and boron carbide (B_4C) powder could be vibration-packed to the desired density of 1.6 g/cc, so that the SS-304 cans to

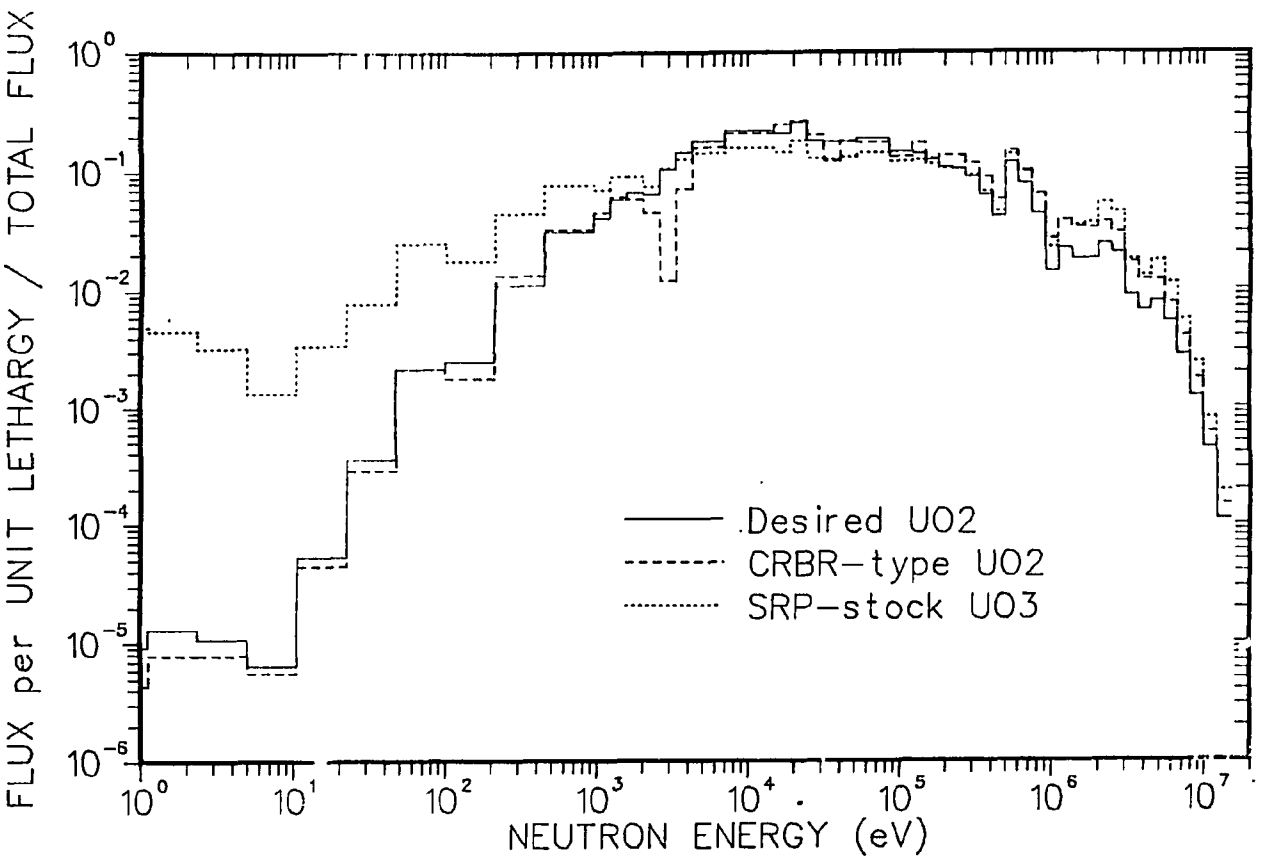

Fig. 3.10. Comparison of leakage spectrum from three blanket assemblies containing alternatives to the desired UO_2 material.

contain the mixture were designed and fabricated with the same thickness dimensions as specified in the CSC.1 design. However, upon attempting to fill the containers, the vendor of the boronated graphite mixture could achieve only a bulk density of 1.0 g/cc.

To determine the effect of several corrective alternatives, 1-D calculations were performed through the shield configuration using different density and different w/o B mixtures. Three alternate cases are compared to the desired mixture in Fig. 3.11 which shows the neutron flux calculated behind the inner shield assembly containing the boronated graphite mixture. The 78 w/o B case (pure B_4C) was clearly not desirable, while the other two alternatives appeared equally acceptable since only the flux normalization was changed. It was therefore decided to use the 25 w/o B mixture at the lower density. However, before filling the slabs with the mixture, the vendor was instructed by ORNL experts on the art of 2-particle vibration packing. Using a technique similar to the loading procedure used to fill the grid-plate shield assemblies in the previous GCFR experiment,[11] a bulk density of 1.4 g/cc was obtained for all of the boronated graphite assemblies. This was quite acceptable for the purposes of the experiment.

3.5.3 Gamma-Ray Filter for ThO_2

One problem which arose during the progress of the experiment was the relatively high gamma-ray activity of the ThO_2 blanket slab. The measured 50 mR/hr activity at the surface of the slabs prohibited the placement of the gamma-ray spectrometer close to the slabs, while other background problems discouraged moving the spectrometer back. A possible alternative was to place a piece of lead or iron between the ThO_2 slabs and the detector.

To investigate the desirability of using such a gamma-ray filter, calculations were performed with 5 and 10 cm of Fe placed against the exit of the ThO_2 configuration. It was decided not to consider a Pb

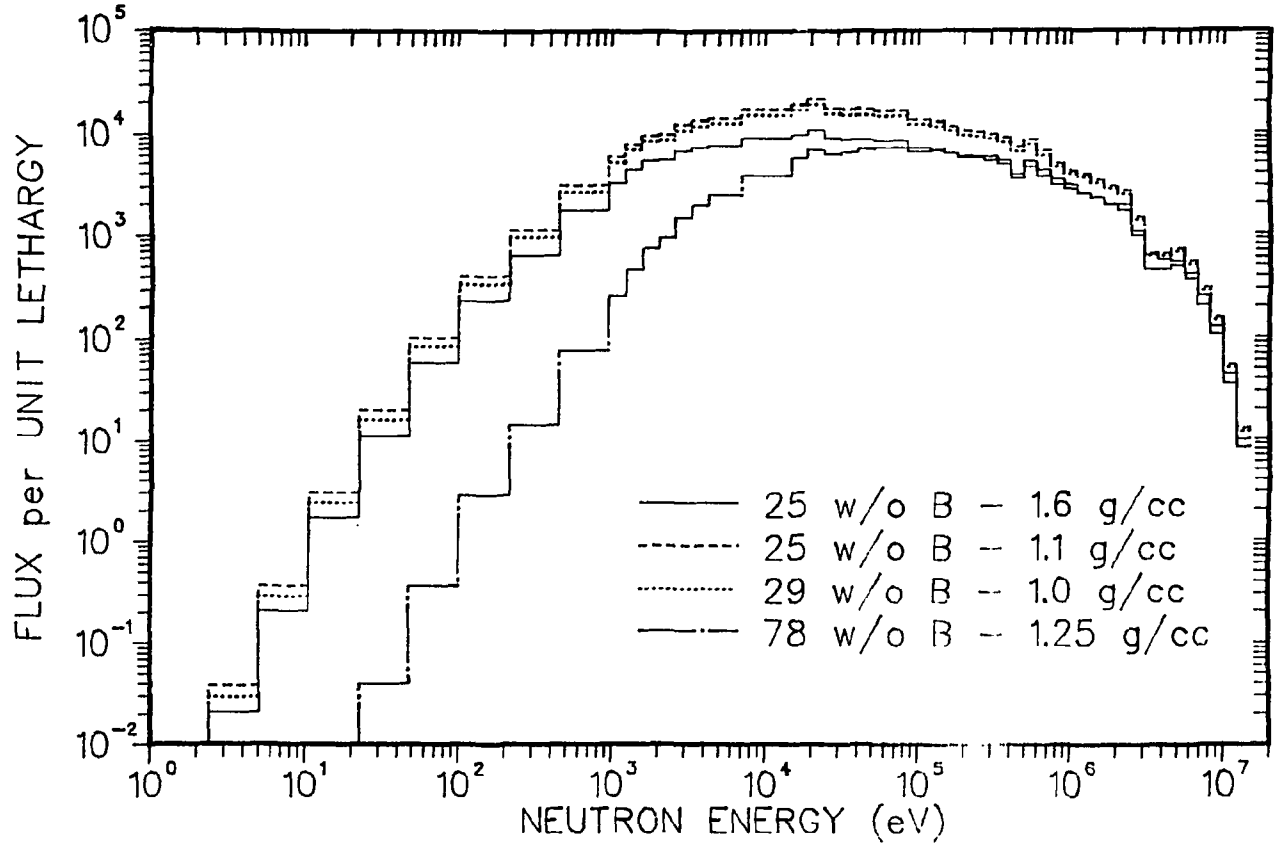

Fig. 3.11. Comparison of leakage spectra from a shield assembly containing several alternative boronated graphite mixtures.

filter since the Pb cross sections are not known as well as iron, which would yield greater uncertainty in the analysis of the experiment. The results of the calculations are shown in Figs. 3.12 and 3.13 which give the neutron and gamma-ray flux behind the 45 cm ThO_2 plus Fe configurations. While the comparison of neutron spectra in Fig. 3.12 tends to discourage the use of the Fe filter, the option was totally discounted by the gamma-ray comparisons in Fig. 3.13. The emergent flux appears to be mostly characteristic of Fe, not ThO_2, which minimizes the reliable inferences that can be made about the ThO_2 data.

The option that was chosen for this problem was to move the spectrometer away from the configuration and to build a concrete house and collimator assembly around the detector to reduce the other background components.

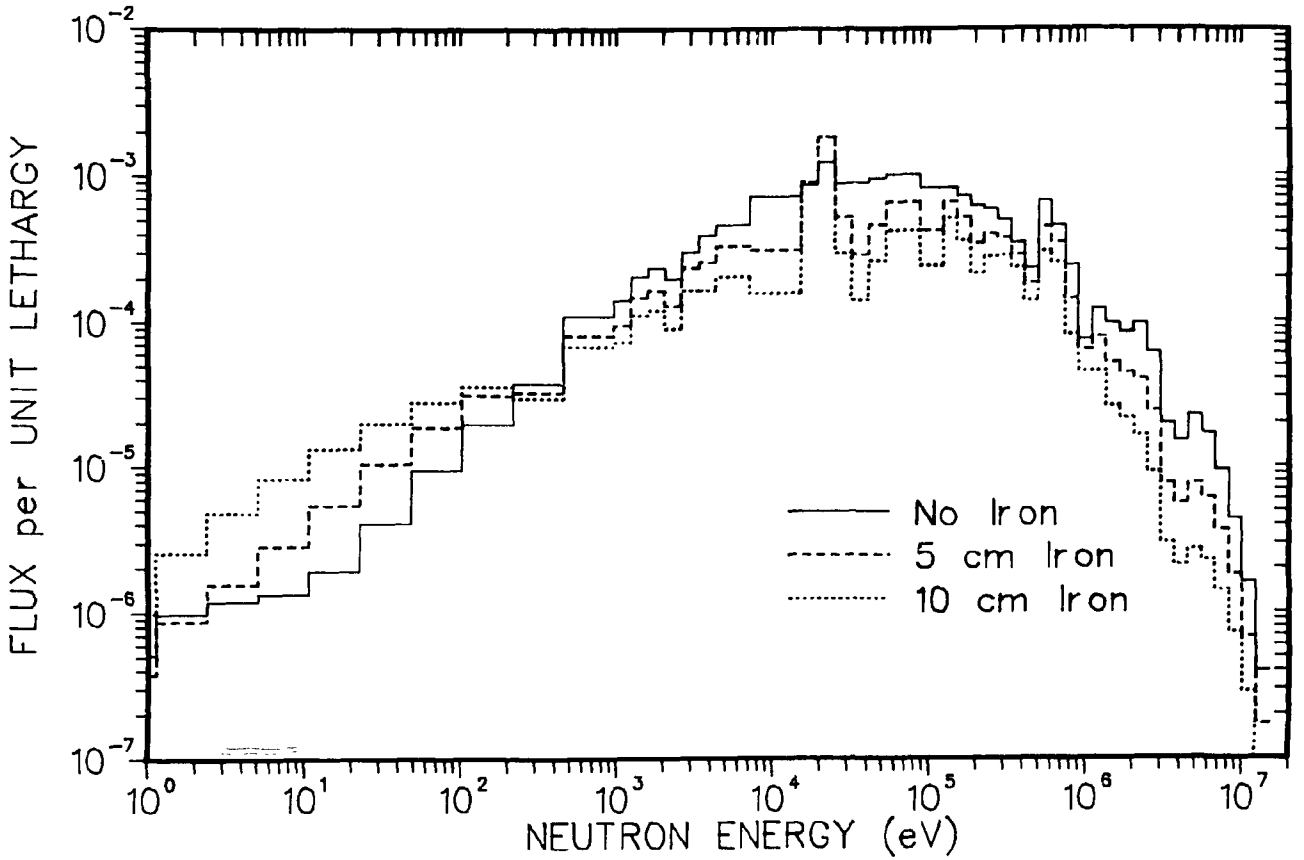

Fig. 3.12. Leakage neutron flux from ThO_2 blanket configuration with no iron, 5 cm and 10 cm of iron behind the ThO_2 slabs.

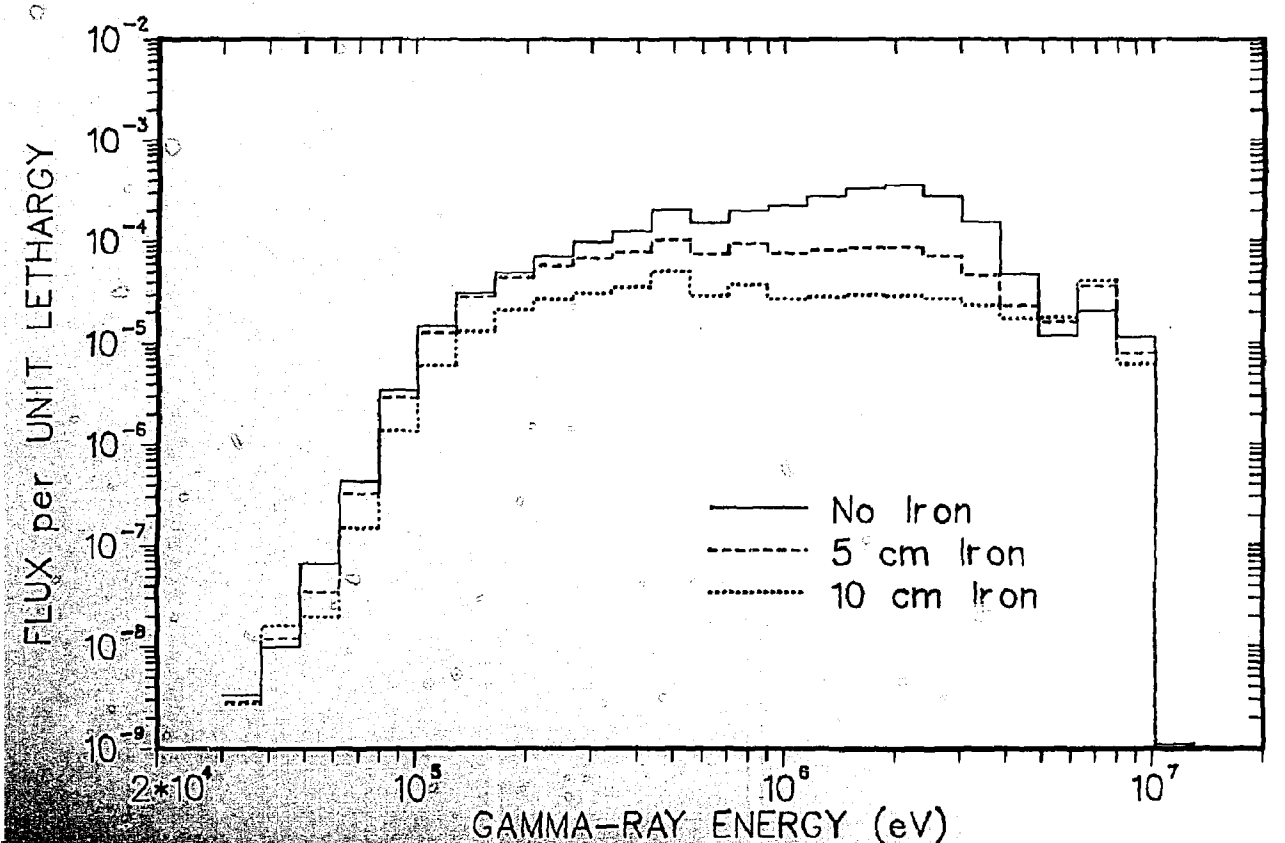

Fig. 3.13. Leakage gamma-ray flux from ThO_2 blanket configuration with no iron, 5 cm and 10 cm of iron behind the ThO_2 slabs.

4.0 EXPERIMENT DESIGN AND SPECIFICATIONS

4.1. TSF Experiment Design

The design of the experiment is similar to previous radial blanket and shielding experiments performed at the Tower Shielding Facility (TSF) for the LMFBR program.[12,13] The TSR II reactor will provide the neutron source[7] which will pass through the large beam collimator and a spectrum modifier to produce the appropriate energy distribution in the neutron flux. The experimental configurations will consist of 150- by 150-cm slabs of blanket and shield material placed perpendicular to the neutron beam centerline. The slabs will be built up in succession with measurements performed behind each configuration. Figure 4.1 shows the experimental geometry for the case of three ThO_2 blanket rows. The concrete which surrounds the configuration provides a biological shield for TSF personnel, while the lithiated paraffin minimizes the contribution of neutrons which reflect from the concrete back into the test assembly. Figure 4.2 shows the experimental geometry for the full blanket and shield mockup.

The experiment will consist of four distinct phases, each phase comprised of several configurations. The first phase will include mockups of a 3-row blanket configuration. The second phase will mockup the currently proposed radial shield design, including both inner shield and outer shield assemblies. The geometry and material specifications for the blanket and shield assemblies are given in Table. 4.1 compared to the specifications for the current GCFR design. Shield design options will be investigated in the third phase which will mockup alternate shield configurations, providing a measured comparison of design performances as well as providing verification of analytic methods and data. Finally, the fourth phase of the experiment will consist of configurations which model the anticipated material and geometric heterogeneities in the

BLANK PAGE

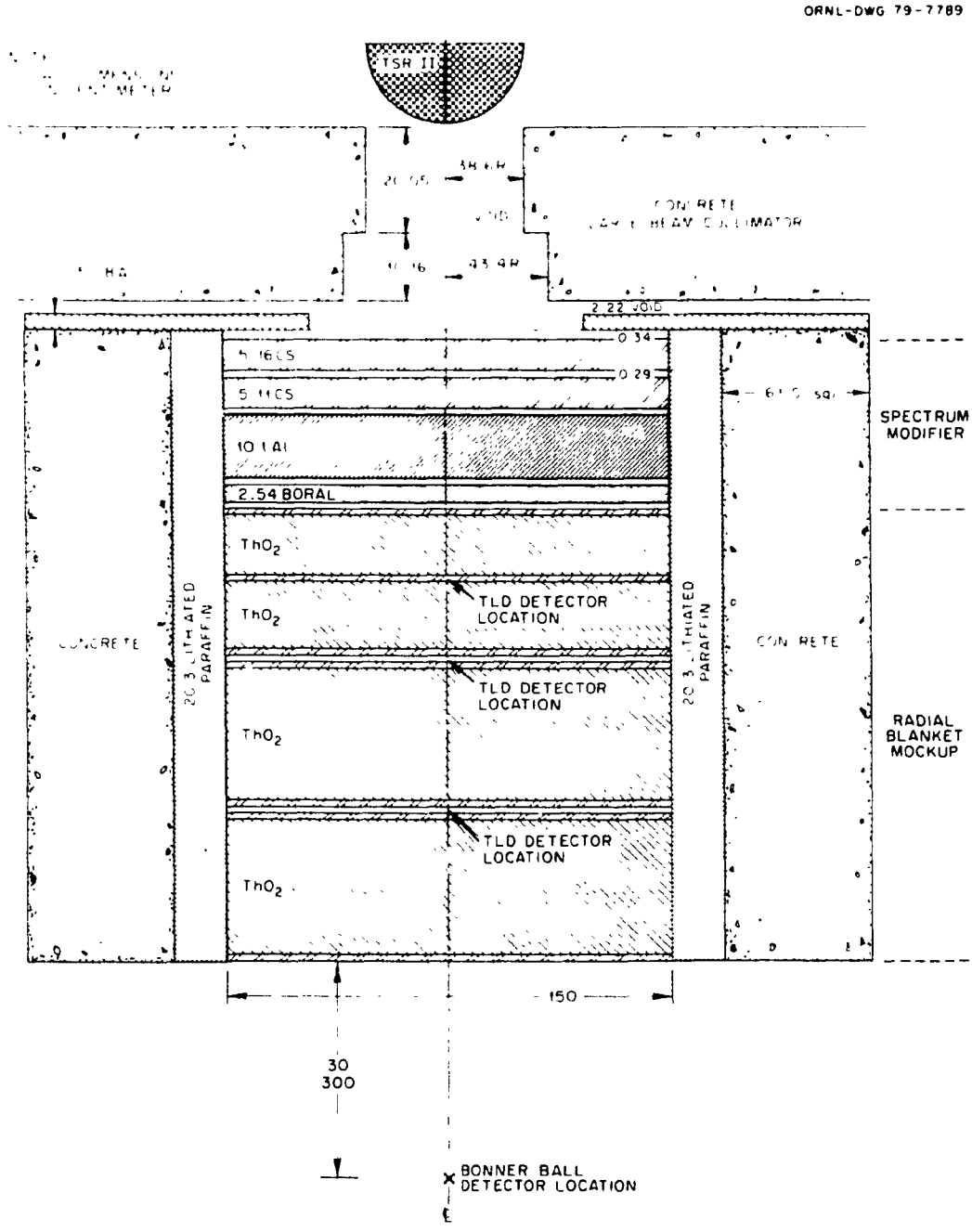

Fig. 4.1. Experimental Geometry for ThO_2 Blanket Configuration.

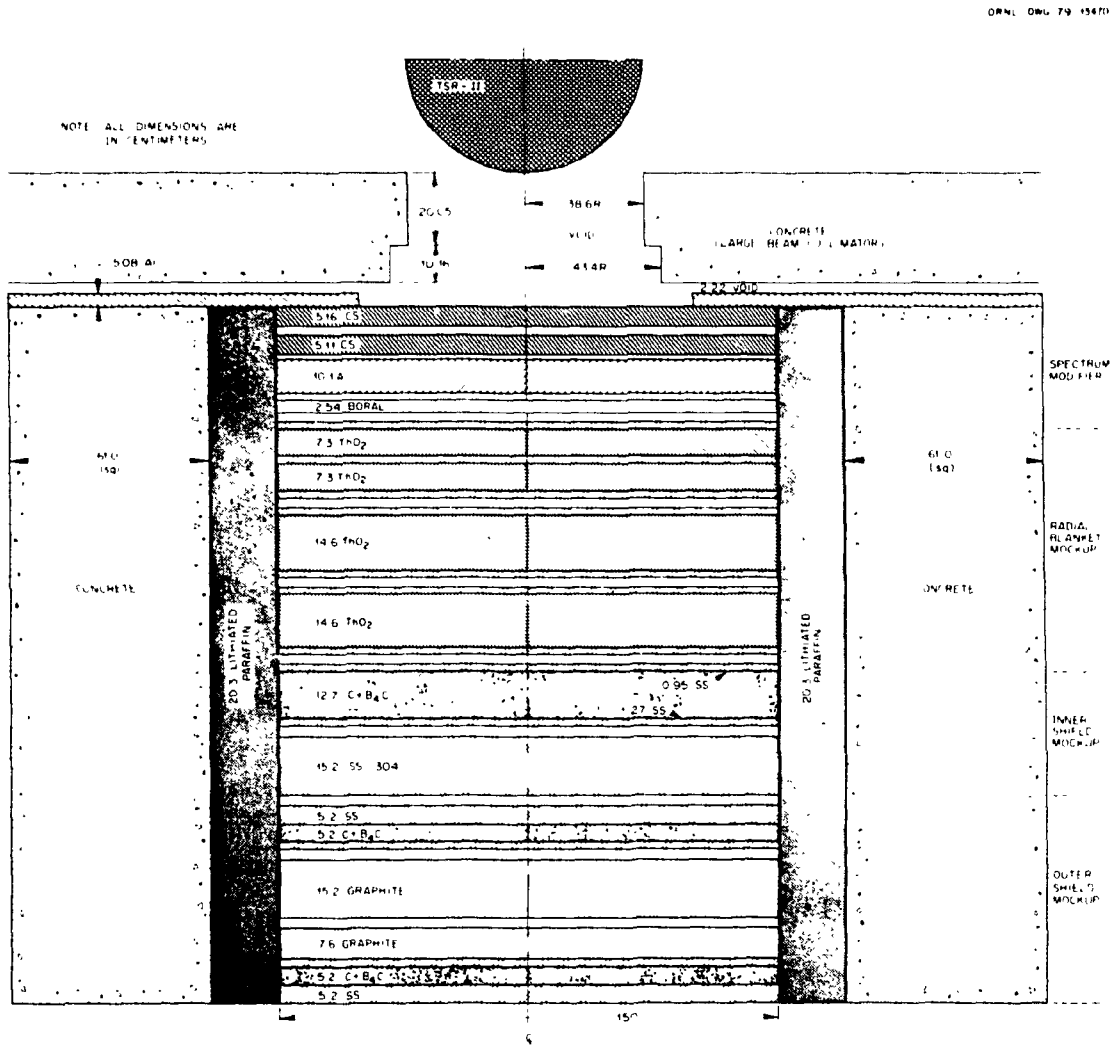

Fig. 4.2. Experimental Geometry for Full Blanket and Shield Configuration.

Table 4.1
Geometry and Material Specifications for
Blanket and Shield Phases of TSF Experiment[a]

Region	Material	Assembly thickness (cm) GCFR[a]	Assembly thickness (cm) Experiment
Radial blanket 1	thorium oxide	15.3[b]	15.2
Radial blanket 2	thorium oxide	15.3	15.2
Radial blanket 3	thorium oxide	15.3	15.2
Helium gap		21.94	
Inner shield 1	stainless steel	0.95	0.95
	boronated graphite	12.78	12.7
	stainless steel	1.27	1.27
Helium gap		5.1	
Inner shield 2	stainless steel	15.0	15.2
Helium gap		5.1	
Outer shield	stainless steel	5.1	5.2
	boronated graphite	5.1	5.1
	stainless steel		0.79
	graphite	22.6	22.9
	stainless steel		0.79
	boronated graphite	5.1	5.1
	stainless steel	5.1	5.2

[a]Corresponds to Conceptual Shielding Configuration I.

[b]Average "radial penetration thickness" which is 0.75 x (diameter across corners).

shield assemblies. Also, several deep penetration through concrete configurations are planned for the fourth phase. Little attention has been given to these configurations since the chance of having sufficient time and funding for these additional items is very remote.

4.2. Detectors

Detectors will include Bonner balls (BB) for integral neutron flux measurements, NE-213 and hydrogen counters for fast neutron spectra measurements, NE-213 for gamma-ray spectra measurements, and thermoluminescent detectors (TLD) for gamma-ray heating measurements. All measurements will be made on the beam centerline, and all detectors except the TLDs will be located behind the configurations.

The energy dependent response functions of the Bonner balls to be used in this experiment are given in Fig. 4.3. A Bonner ball is a spherical BF_3 counter surrounded by spherical shells of polyethelene of various thicknesses. Additionally, all except the bare BF_3 have an outer cadmium cover. The thickness of the polyethylene and hence the overall size of the Bonner ball determines the energy range of maximum sensitivity. As seen in Fig. 4.3, the 3", 6", and 10" Bonner balls respond mainly to epithermal, total, and fast neutron flux, respectively.

The response of a CaF_2 TLD is given in Fig. 4.4 compared to the gamma-ray heating response of type 316 stainless steel. The two responses are very similar except for the lower energy gamma rays.

The NE-213 scintillation detector will provide neutron spectrum measurements above 0.6 MeV and gamma-ray spectrum measurements above 1 MeV. Pulse shape discrimination methods will be used to collect the neutron and gamma-ray data simultaneously, and pulse height unfolding techniques will be used to obtain absolute flux spectra. The multiple-pressure hydrogen counters will be used and unfolded to obtain neutron spectra from 10 keV to 2 MeV.

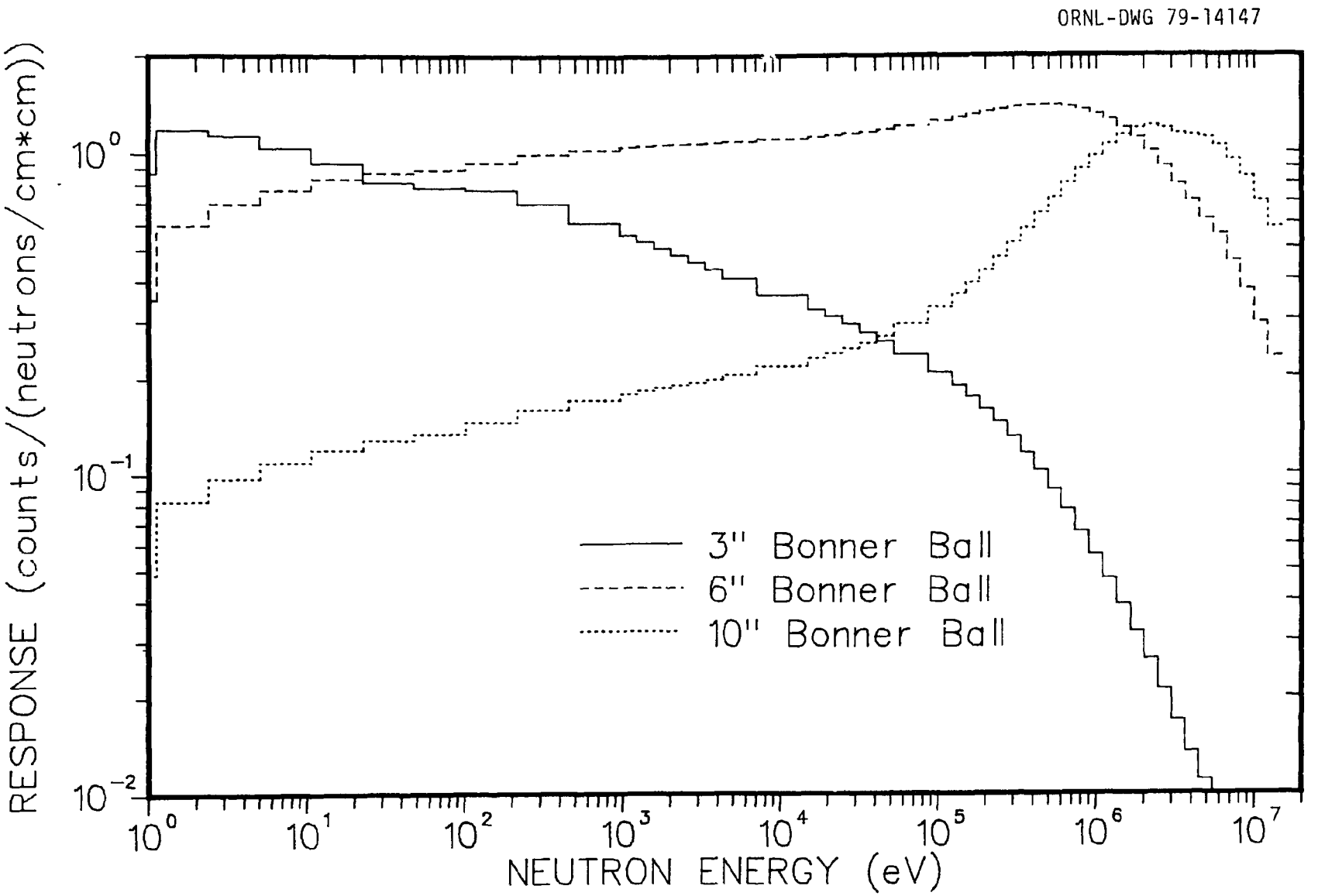

Fig. 4.3. Response functions for Bonner balls to be used in this experiment.

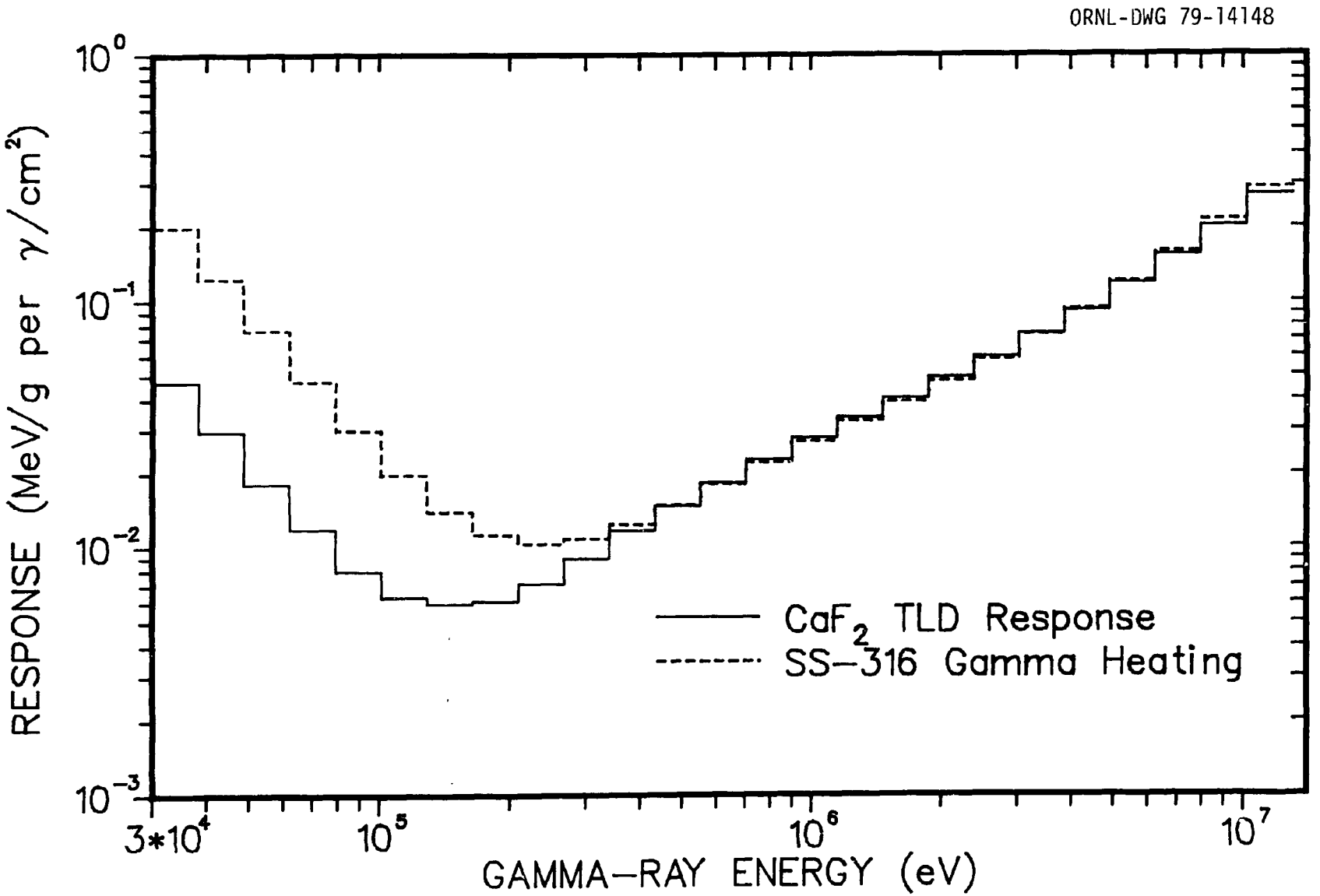

Fig. 4.4. Response function of TLD compared to type-316 stainless steel gamma-ray heating response.

4.3. Measurement Specifications

A detailed description of all configurations and the corresponding measurements is given below. The specifications are summarized in Table 4.2. The priorities were assigned in agreement with GAC and represent an importance ranking. It is expected that all of Priority 1 will be completed in the original time and cost schedule, but that additional funds will be required for the "wish list" items in Priority 2 and 3.

I. ThO_2 Blanket Configurations (Priority 1A)

A. Spectrum Modifier (SM) (10.2-cm Fe + 8.9-cm Al + 2.54 Boral)

1. 3-, 6-, and 10-in. Bonner ball on centerline at 30.5 cm.
2. 3-, 6-, and 10-in. Bonner ball at 304.8 cm and NE213 or Hydrogen counter location.
3. NE213 on centerline as close as feasible.
4. Hydrogen counters (1D) at NE213 location. (If NE213 run not feasible do hydrogen counters as close as feasible.)

B. Spectrum Modifier + 1.27-cm void + 7.62-cm ThO_2 slab

1. 3-, 6-, and 10-in. Bonner ball on centerline at 30.5 cm.
2. 3-, 6-, and 10-in. Bonner ball on centerline at 304.8 cm.

C. Spectrum Modifier + 1.27-cm void + 7.62-cm ThO_2 + 1.27-cm void + 7.62-cm ThO_2

1. 3-, 6-, and 10-in. Bonner ball on centerline at 30.5 cm.
2. 3-, 6-, and 10-in. Bonner ball on centerline at 304.8 cm.

D. Spectrum Modifier + 1.27-cm void + 7.62-cm ThO_2 + 1.27-cm void + 7.62-cm ThO_2 + 1.27-cm void + 15.2-cm ThO_2

1. 3-, 6-, and 10-in. Bonner ball on centerline at 30.5 cm.
2. 3-, 6-, and 10-in. Bonner ball on centerline at 304.8 cm and at NE213 location.
3. NE213 on centerline as close as feasible.
4. Hydrogen counters (1D) at NE213 location.
5. TLD measurements on centerline in each void.

Table 4.2

Summary of Configurations and Measurements

for GCFR Radial Blanket and Shield Experiments

No.	Configuration	Priority	Description[a]	Measurements[b]
1	I.A	1A	Spectrum modifier	BB, S
2	I.B	1A	1/2 Th blanket row	BB
3	I.C	1A	1 Th blanket row	BB
4	I.D	1A	2 Th blanket rows	BB, S, TLD
5	I.E	1A	3 Th blanket rows	BB, S, TLD
6	I.F	1A	3 Th blanket rows + reflector	TLD
7	II.A	1A	3 U blanket rows	BB, S, TLD
8	II.B	1A	3 U blanket rows + inner radial shields	BB, S
9	III.A	1B	Inner radial shield row 1	BB, S
10	III.B	1B	Inner radial shield row 1 & 2	BB, S
11	IV.A	1C	Inner + 1/3 outer radial shield	BB
12	IV.B	1C	Inner + 2/3 outer radial shield	BB
13	IV.C	1C	Inner + outer radial shield	BB, S
14	IV.D	1C	Radial shield + PCRV	BB, TLD
15	V.A	1D	Graphite + SS inner shield	BB, TLD
16	V.B	1D	SS + SS inner shield	BB, TLD
17	V.C	1D	SS + (C + B_4C) + SS shield	BB, TLD
18	VI.A	2	Graphite with 2" SS-304	HB
19	VI.A	2	Graphite with 1" SS-304	HB
20	VI.A	2	Graphite with 1/4" gap	HB
21	VI.A	2	Graphite with 1/2" gap	HB
22	VI.B	2	SS-304 with no gap	HB
23	VI.B	2	SS-304 with 1/4" gap	HB
24	VI.B	2	SS-304 with 1/2" gap	HB
25	VI.B	2	SS-304 with 1" gap	HB
26	VII.A	3	CS + 6" concrete	BB, S
27	VII.B	3	CS + 12" concrete	BB, S
28	VII.C	3	CS + 24" concrete	BB, S
29	VII.D	3	CS + 36" concrete	BB, S

[a] Inner and outer shields refer to CSC.1 design; SS = stainless steel; CS = carbon steel.

[b] BB = Bonnerball; S = spectrometer; TLD = thermoluminescent detector; HB = Hornyak button.

E. Spectrum Modifier + 1.27-cm void + 15.2-cm ThO_2 + 1.27-cm void + 7.62-cm ThO_2 + 1.27-cm void + 7.62-cm ThO_2 + 1.27-cm void + 15.2-cm ThO_2

1. 3-, 6-, and 10-in. Bonner ball on centerline at 30.5 cm.
2. 3-, 6-, and 10-in. Bonner ball on centerline at 304.8 cm at NE213 location.
3. NE213 on centerline as close as feasible.
4. Hydrogen counters (1D) at NE213 location.
5. TLD measurements on centerline in each void.

F. Spectrum Modifier + 1.27-cm void + 15.2-cm ThO_2 + 1.27-cm void + 15.2-cm ThO_2 + 1.27-cm void + 7.62-cm ThO_2 + 1.27-cm void + 7.62-cm ThO_2 + 1.27-cm void + 25.4-cm Fe

1. TLD measurements on centerline in each void.

II. UO_2 Blanket Configuration (Priority 1A)

A. Spectrum Modifier + 1.27-cm void + 10.2-cm (UO_2 + Na) + 1.27-cm void + 10.2-cm (UO_2 + Na) + 1.27-cm void + 10.2 cm (UO_2 + Na)

1. 3-, 6-, and 10-in. Bonner ball on centerline at 30.5 cm.
2. 3-, 6-, and 10-in. Bonner ball on centerline at 304.8 cm and at NE213 location.
3. NE213 on centerline as close as feasible.
4. Hydrogen counters (1D) at NE213 location.
5. TLD measurements on centerline in each void.

B. Spectrum Modifier + 1.27-cm void + 10.2-cm (UO_2 + Na) + 1.27-cm void + 10.2-cm (UO_2 + Na) + 1.27-cm void + 10.2-cm (UO_2 + Na) + {0.95-cm SS + 12.7-cm (B_4C + C) + 1.27-cm SS} container + 15.2-cm SS

1. 3-, 6-, and 10-in. Bonner ball on centerline at 30.5 cm.
2. 3-, 6-, and 10-in. Bonner ball on centerline at 304.8 cm and at NE213 location.
3. NE213 on centerline at feasible location.
4. Hydrogen counters (1D) at NE213 location.

III. Inner Radial Shield Configurations (Priority 1B)

A. Spectrum Modifier + 45.7-cm ThO_2 + {0.95-cm SS + 12.7-cm (B_4C + C) + 1.27-cm SS} container

1. 3-, 6-, and 10-in. Bonner ball on centerline at 30.5 cm.
2. 3-, 6-, and 10-in. Bonner ball on centerline at 304.8 cm and at NE213 location.
3. NE213 on centerline as close as feasible.
4. Hydrogen counters (1D) at NE213 location.

B. Spectrum Modifier + 45.7-cm ThO_2 + {0.95-cm SS + 12.7-cm (B_4C + C) + 1.27-cm SS} container + 15.2-cm SS

1. 3-, 6-, and 10-in. Bonner ball on centerline at 30.5 cm.
2. 3-, 6-, and 10-in. Bonner ball on centerline at 304.8 cm and at NE213 location.
3. NE213 on centerline as close as feasible.
4. Hydrogen counters (1D) at NE213 location.

IV. Outer Radial Shield Configurations (Priority 1C)

A. Spectrum Modifier + 45.7-cm ThO_2 + {0.95-cm SS + 12.7-cm (B_4C + C) + 1.27-cm SS} container + 1.27-cm void + 15.2-cm SS + 1.27-cm void + 4.45-cm SS + {0.8-cm SS + 5.1-cm (B_4C + C) + 0.8-cm SS} container

1. 3-, 6-, and 10-in. Bonner ball on centerline at 30.5 cm.
2. 3-, 6-, and 10-in. Bonner ball on centerline at 304.8 cm.

B. Spectrum Modifier + 45.7-cm ThO_2 + {0.95-cm SS + 12.7-cm (B_4C + C) + 1.27-cm SS} container + 1.27-cm void + 15.2-cm SS + 1.27-cm void + 4.45-cm SS + {0.8-cm SS + 5.1-cm (B_4C + C) + 0.8-cm SS} container + 22.9-cm graphite

1. 3-, 6-, and 10-in. Bonner ball on centerline at 30.5 cm.
2. 3-, 6-, and 10-in. Bonner ball on centerline at 304.8 cm.

C. Repeat B + {0.8-cm SS + 5.1-cm (B_4C + C) + 0.8-cm SS} container + 4.45-cm SS

1. 3-, 6-, and 10-in. Bonner ball on centerline at 18 cm and 30.5 cm.
2. 3-, 6-, and 10-in. Bonner ball on centerline at 304.8 cm and at NE213 location.

3. NE213 on centerline as close as feasible.
4. Hydrogen counters (1D) at NE213 location.

D. Repeat C + 35.6-cm void + 2.54-cm Fe + 61-cm concrete

1. 3-, 6-, and 10-in. Bonner ball on centerline in 35.6-cm void at 18 cm behind the SS.
2. TLD in front of 15.2-cm SS.
3. TLD behind 15.2-cm SS.
4. TLD in front of 1.9-cm SS.

V. Alternate Inner Radial Shield Configurations (Priority 1D)

A. Spectrum Modifier + 45.7-cm ThO_2 + 1.27-cm void + 15.2-cm graphite + 1.27-cm void + 15.2-cm SS

1. 3-, 6-, and 10-in. Bonner ball at 30.5 cm and 304.8 cm.
2. TLD on centerline in both voids.

B. Spectrum Modifier + 45.7-cm ThO_2 + 1.27-cm void + 15.2-cm SS + 1.27-cm void + 15.2-cm SS

1. 3-, 6-, and 10-in. Bonner ball on centerline at 30.5 cm and 304.8 cm.
2. TLDs on centerline in the voids.

C. Spectrum Modifier + 45.7-cm ThO_2 + 1.27-cm void + 15.2-cm SS + 1.27-cm void + {0.95-cm SS + 12.7-cm (B_4C + C) + 1.27-cm SS} container + 1.27-cm void + 15.2-cm SS

1. 3-, 6-, and 10-in. Bonner ball on centerline at 30.5 cm and 304.8 cm.
2. TLDs on centerline in the voids.

VI. Heterogeneous Shield Configurations (Priority 2)

A. Bare beam + two 20.3-cm-thick graphite slabs (use pieces from Carborundum or our own supply) placed perpendicular to the beam centerline in the same vertical plane against the reactor shield (edge to edge) with a vertical spacing between them according to the following:

a) 5.1-cm SS (same depth as graphite)
b) 2.54-cm SS (same depth as graphite)
c) 0.635-cm void
d) 1.27-cm void

1. Hornyak button (0.635 cm) traverses with the horizontal plane directly behind each of the configurations.
2. Hornyak button (0.635 cm) traverses in the horizontal plane at 30.5 cm behind each of the configurations.

B. Bare beam + two 20.3-cm-thick SS slabs placed perpendicular to beam centerline in the same vertical plane against the reactor shield (edge to edge) with a vertical spacing between them according to the following:

a) no void
b) 0.635-cm void
c) 1.27-cm void
d) 2.54-cm void

1. Hornyak button (0.635 cm) traverses in the horizontal plane directly behind each of the configurations.
2. Hornyak button (0.635 cm) traverses in the horizontal plane at 30.5 cm behind each of the configurations.

VII. PCRV Configurations (Priority 3)

A. 5.1-cm Fe + 15.2-cm concrete

1. 3-, 6-, and 10-in. Bonner ball on centerline at 30.5 cm.
2. 3-, 6-, and 10-in. Bonner ball on centerline at 304.8 cm and NE213 location.
3. NE213 as close as feasible.

B. 5.1-cm Fe + 30.5-cm concrete

1. 3-, 6-, and 10-in. Bonner ball on centerline at 30.5 cm.
2. 3-, 6-, and 10-in. Bonner ball on centerline at 304.8 cm and NE213 location.
3. NE213 as close as feasible.
4. Hydrogen counters (1D) at NE213 location.

C. 5.1-cm Fe + 61-cm concrete

1. 3-, 6-, and 10-in. Bonner ball on centerline at 30.5 cm.
2. 3-, 6-, and 10-in. Bonner ball on centerline at 304.8 cm and NE213 location.
3. NE213 as close as feasible.
4. Hydrogen counters (1D) at NE213 location.

D. 5.1-cm Fe + 91.4-cm concrete

1. 3-, 6-, and 10-in. Bonner ball on centerline at 30.5 cm.
2. 3-, 6-, and 10-in. Bonner ball on centerline at 304.8 cm and NE213 location.
3. NE213 as close as feasible.
4. Hydrogen counters (1D) at NE213 location.

4.4. Quality Assurance Procedures

The preanalysis of this experiment has followed practices for the implementation of required DOE and/or other Quality Assurance Standards. By official agreement, the GCFR program follows ANSI N45.2.

REFERENCES

1. General Atomic Co. Project Staff, "300-MW(e) Gas-Cooled Fast Breeder Reactor Demonstration Plant," General Atomic Company Report GA-A13045 (1974).

2. R. G. Perkins, D. T. Ingersoll, C. J. Hamilton, "GCFR Radial Blanket and Shield Experiment Requirements," Unpublished report, February 28, 1979.

3. "Conceptual Shielding Configuration I, "Letter to Dr. U. Gat from J. H. Broido, June 27, 1978.

4. Letter with enclos[illegible] from C. J. Hamilton to D. E. Bartine regarding a description of the core and blanket model for the End of Equilibrium Cycle Shielding Core Model A, (March 11, 1978). (Also referenced in GA quarterly progress report.)

5. W. W. Engle, Jr., "A User's Manual for ANISN — A One-Dimensional Discrete Ordinates Transport Code with Anisotropic Scattering," K-1693 (1967).

6. Uri Gat and P. R. Kasten, "Gas-Cooled Fast Reactor Program Annual Progress Report for Period Ending December 31, 1977," Irene Brogden, ed., Oak Ridge National Laboratory Report ORNL-5426 (August 1978).

7. R. E. Maerker, F. J. Muckenthaler, "The Absolute Neutron Spectrum Emerging Through the Large Beam Collimator from the TSR-II Reactor at the Tower Shielding Facility," ORNL/TM-5183 (1976).

8. D. E. Bartine, F. R. Mynatt, E. M. Oblow, "SWANLAKE, A Computer Code Utilizing ANISN Radiation Transport Calculations for Cross Section Sensitivity Analysis," ORNL/TM-3809 (1973).

9. M. L. Williams and W. W. Engle, Jr., "The Concept of Spatial Channel Theory Applied to Reactor Shielding Analysis," Nucl. Sci. and Eng., 62, pp. 92-104 (1977).

10. M. L. Williams and F. B. Sadler, "The FANG Angular Folding Code for Channel Theory Analysis," ORNL/TM-5228.

11. F. J. Muckenthaler, J. L. Hull, and J. J. Manning, "The GCFR Grid Plate Shield Design Confirmation Experiment, ORNL/TM-6580 (January 1979).

12. R. E. Maerker, "Analysis of TSF Experiments on Radiation Heating in a Stainless Steel-Sodium CRBR Radial Shield Mockup Using a 32-Inch Diameter Collimated Beam Source, ORNL/TM-5992.

13. R. E. Maerker and F. J. Muckenthaler, "Measurements and Analysis of the CRBR Inconel-Stainless Steel Radial Shield Experiment, ORNL/TM-5346.